


A review of garnet deposits in western and southern Iran

Fatemeh Nouri^a, Robert J. Stern^b and Hossein Azizi ^a

^aDepartment of Mining, Faculty of Engineering, University of Kurdistan, Sanandaj, Iran; ^bGeosciences Department, University of Texas at Dallas, Richardson, TX, 75083-0688, USA

ABSTRACT

Garnets show wide ranges of chemical compositions and are key minerals for reconstructing the thermodynamic evolution of metamorphic terranes. The properties of garnets – including Mohs hardness ~7, lack of cleavage, vitreous luster and multiple colors – also makes them useful as semi-gemstones. Garnets are widespread accessory minerals in igneous and metamorphic rocks of western and southern Iran and are especially abundant in skarns and regional metamorphic rocks. 45 garnet deposits of western and southern Iran show six associations: (1) skarn (35 locations); (2) peraluminous granitoid and rhyolite (4 locations); (3) alkaline granite (1 location); (4) metamorphic rocks (3 locations); and (5) ophiolites (2 locations). Distinct garnet compositions are found in each association: mostly grossular-andradite in skarn, Ti-andradite in alkaline granite, almandine in peraluminous granite and volcanic rocks, almandine-grossular in metamorphic rocks and andradite-uvarovite associated with ophiolites. Western and southern Iran garnets are mostly related to skarns around Cenozoic granitoid intrusions. Ti-rich garnet formed at the expense of clinopyroxenites in alkaline igneous complexes due to alkaline metasomatism. These associations are useful for understanding garnet semi-gemstone deposits in western and southern Iran.

ARTICLE HISTORY

Received 2 July 2020
Accepted 8 October 2020

KEYWORDS

Semi-gemstone; garnet; metasomatism; granite; skarn deposit; iran

1. Introduction

1.1. Garnet definition

Garnet is a silicate mineral with Mohs hardness between 6.5 and 7.5 and is generated in a wide range of igneous and metamorphic rocks from the mantle to the crust (Meen and Tushigham 1968; Pearl 1975; Sinkankas 1961, 1972; Smith and Phillips 1972; Stockton and Manson 1982; Stockton and Mason 1982; Webster 1983; Baxter *et al.* 2013). In terms of mineralogy, garnets are orthosilicates, with isometric (cubic) structure and show a wide range of compositions and colors. They exhibit wide chemical variability with a general formula of $X_3Y_2(SiO_4)_3$, where X = divalent cations Mg, Fe, Mn, and Ca and Y – trivalent Al, Fe, and Cr. These combinations result in different endmembers, the most common of which are pyrope (Mg, Al), almandine (Fe^{+2} , Al), spessartine (Mn, Al), grossular (Ca, Al) and andradite (Ca, Fe^{+2}) (Sinkankas 1961, 1972; Smith and Phillips 1972; Pearl 1975; Stockton and Manson 1982; Webster 1983). Garnets with Al in the Y site are known as Pyralspite whereas those with Ca in the Y site are called Ugrandite. Garnets have low contents of SiO_2 (~40 wt. %) and tend to form in high-T (>600°C) silica-deficient environments. Metamorphic garnet is found in almost any silica-poor protolith, from lower greenschist facies

grade to ultra-high-temperature (UHT) granulites and ultra-high pressure (UHP) eclogites. Garnet occasionally forms in igneous rocks, for example in peraluminous granites. Garnets are also found in mantle peridotites.

1.2. History of garnet semi-gemstone deposits

Garnets are one of the oldest known semi-gemstones, having adorned many royal necks and wrists. They have been found in many ancient Greek, Egypt and Iranian ruins (Ghorbani 2003). The jewelry and gemstone industry in Iran has a history of several thousand years, and Iranian interest in jewelry and gemstones are an important part of this ancient civilization (Meen and Tushigham 1968; Ghorbani 2003). Ancient Iranians used garnets as gem and stone for their sling bows (Meen and Tushigham 1968; Ghorbani 2003). They believed that the color of the garnet had magical properties and bestowed luck on the possessor, in addition to their material value (Ghorbani 2003).

There is much we can learn about the P-T-t evolution of Iran from studying garnets and garnetiferous metamorphic rocks (Baxter *et al.* 2013). There is also significant economic opportunity for mining garnets as semi-gemstones and other purposes in Iran, but realizing this potential is difficult because there are no systematic

overview of these deposits that can guide exploration and exploitation. Here, we summarize the distribution of garnet semi-gemstones in western and southern Iran from the northwest to southeast. These deposits are associated with two well-defined geologic tracts – the Sanandaj-Sirjan Zone and Urumieh-Dokhtar magmatic belt – that experienced pervasive magmatism, metamorphism, and deformation at different times. Both have abundant granitoids, metamorphics, and skarn deposits that contain pockets of garnet semi-gemstones. There are many reports on the garnet deposits of this region (Takab, Baba Nazar, Bagh borj, Soghan, Panah Kuh, Khut, Qazan, Joveinan, Choogan, Fesharak, Baghin, Khajoo, Kouh Gabri) (Douman and Dirlam 2004; Moradian *et al.* 2005; Abedpour and Tarrah 2010; Abedpour *et al.* 2013; Montaseri 2011; Peighambari *et al.* 2012; Zahedi *et al.* 2013; Zahedi *et al.* 2014; Alipour *et al.* 2016; Malehmir 2016; Ayati 2012, 2017; Hajialioghli 2018; Chavideh *et al.* 2018; Tabatabaei Manesh *et al.* 2018), but there is not any systematic overview. This study aims to aid overcome this shortcoming by summarizing what is known about garnet semi-gemstones of southern and western Iran.

2. Geological background

Iran is part of the Alpine-Himalayan orogen and is part of the Eurasian plate, squeezed by the Arabian plate to the southwest. Iran is divided in different structural zones (Stöcklin and Nabavi 1973), reflecting the effects of Neo-Tethys Ocean subduction since the Late Cretaceous. Huge volumes of magmatic and metamorphic rocks were produced in western and southern Iran (Berberian and King 1981; Ghazi and Hassanipak 1999; Agard *et al.* 2005, 2011; Azizi and Moinevaziri 2009; Azizi *et al.* 2011; Azizi and Asahara 2013; Sacconi *et al.* 2014). The main magmatic and metamorphic activity was overprinted on the Cadomian (Late Ediacaran – Early Cambrian) basement (Stöcklin 1968; Nadimi 2007) but the igneous rocks are mainly Mesozoic or younger. Paleozoic basement is also observed in northern, central and northwestern Iran (Sengör 1987; Stampfli 2000; Zanchetta *et al.* 2009; Zanchi *et al.* 2009; Badr *et al.* 2018).

Southern and western Iran geology is dominated by the Zagros orogen. This consists of three main parts from SW to NE (Figure 1): 1) Zagros fold-thrust belt (ZFTB), 2) Sanandaj-Sirjan Zone (SaSZ) and 3) Urumieh-Dokhtar magmatic assemblage (UDMA) (Stöcklin 1968; Berberian and King 1981; Alavi 1994; Agard *et al.* 2005, 2011). In the Zagros orogen, semi-gemstones occur in two main tectono-magmatic units, the Sanandaj-Sirjan Zone and Urumieh-Dokhtar magmatic belt. The SaSZ extends from southeast to northwest Iran (Figure 1).

SaSZ was an important site of igneous and metamorphic activity in especially Jurassic time and includes many granitoid intrusions (Agard *et al.* 2005; Esmaeily *et al.* 2005; Davoudian *et al.* 2008; Aghazadeh *et al.* 2010; Mahmoudi *et al.* 2011; Azizi *et al.* 2011, 2015). Earlier workers interpreted SaSZ igneous activity as reflecting a magmatic arc but it has recently been re-interpreted as a continental rift (Azizi and Stern 2019).

The Urumieh-Dokhtar magmatic assemblage (UDMA; Figure 1) lies north of the SaSZ, where it forms a distinct, elongated intrusive-extrusive belt (Berberian and Berberian 1981; Alavi 1994). The UDMA marks the magmatic front of the Late Cretaceous – Cenozoic magmatic arc formed by subduction of Neo-Tethys beneath Iran (Figure 1). The UDMA is dominated by extrusive and intrusive rocks of Paleogene age and associated volcanoclastic successions. The volcanic sequences are more than 4 km thick and occur as lava flows, pyroclastic layers, tuff and ignimbrites (Stöcklin 1968; Berberian and Berberian 1981; Alavi 2007). UDMA igneous rocks can be tholeiitic, calc-alkaline or K-rich. Paleogene UDMA volcanics and sedimentary rocks formed near sea level, indicating subsidence associated with extension (Vincent *et al.* 2005; Ballato *et al.* 2011; Verdel *et al.* 2011), including formation of Eocene core complexes in Central Iran (Moritz *et al.* 2006; Verdel *et al.* 2011). A magmatic flare-up occurred in Eocene time, ceasing at 37 Ma (Verdel *et al.* 2011); Oligocene magmatism changed to OIB-like volcanism that reflected asthenospheric melting (Verdel *et al.* 2011). The youngest UDMA rocks consist of alkaline lava flows and pyroclastics of Pliocene and Quaternary age (Berberian and Berberian 1981). Figure 1 illustrates the location of the garnet semi-gem deposits in relation to geological structure of the area.

3. Garnet semi-gemstone locations in western and southern Iran

There are 45 significant deposits of garnet in the study area, defining a belt that is about 1500 km long and 150 km across Table 1. These are subdivided on a basis of location into five districts, from NW to SE: Azerbaijan (17 deposits), Qom-Zanjan (3 deposits), Isfahan (8 deposits), Yazd (10 deposits) and Kerman (7 deposits) (Figure 1). These formed in five main tectono-magmatic settings: (1) skarn; (2) peraluminous granitoids and rhyolites; (3) alkaline rocks; (4) metamorphic rocks; and (5) ophiolites. These tectono-magmatic setting are described further in Section 4. Skarn deposits are especially important in the Azerbaijan, Isfahan, and Yazd districts; the Qom-Zanjan and Kerman districts have fewer and more variable types of deposits. Seven deposits belong to SaSZ and 38 belong to UDMA. All garnet deposits in the Azerbaijan district and some garnet

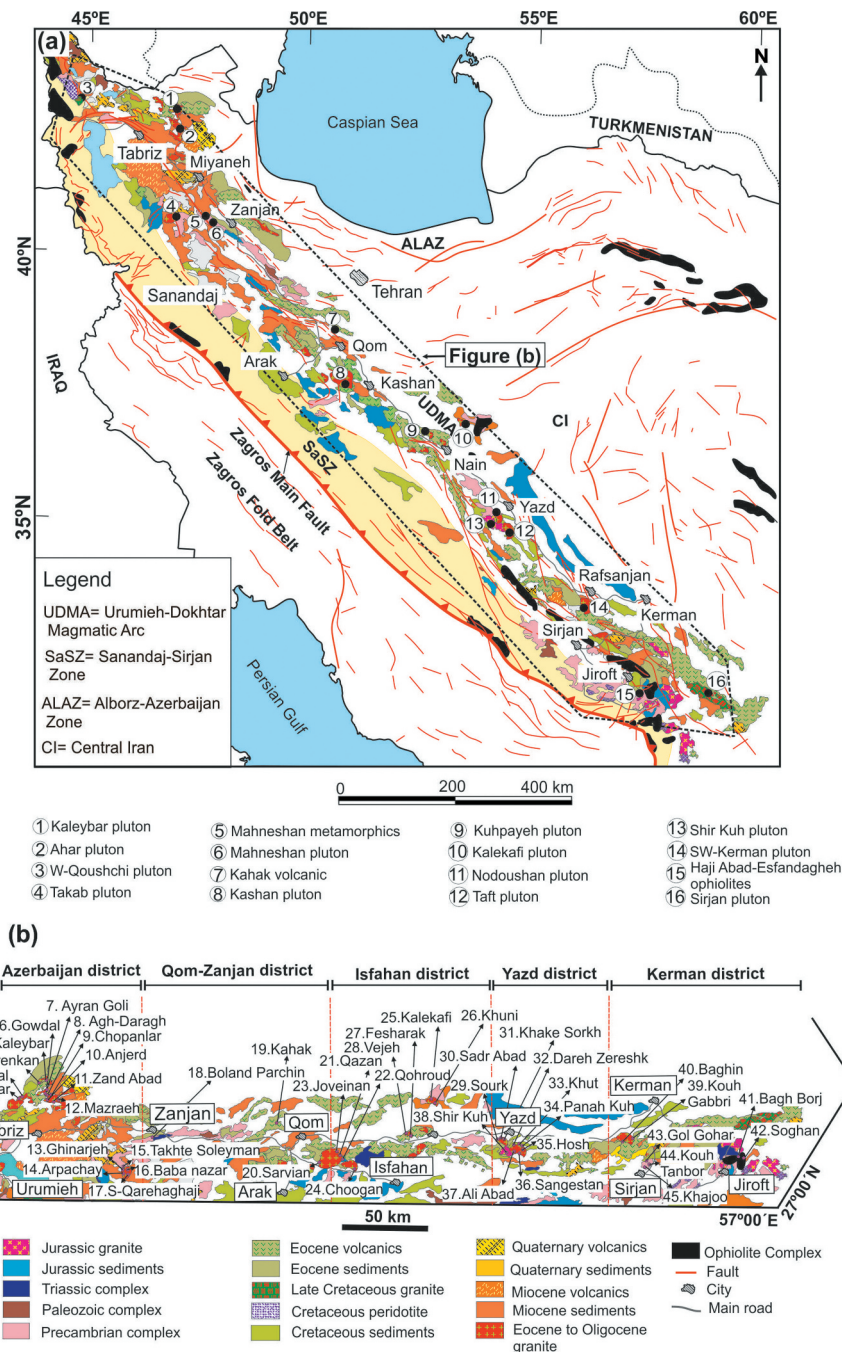


Figure 1. (a) Simplified geological map of Iran (modified from Stöcklin, 1968). (b) Simplified geology map of western Iran which shows the location of garnet semi-gemstone deposits and their host rocks (modified from Stöcklin, 1968).

deposits in the Kerman district (Gol Gohar, Kouh Tanbor, Khajoo, Soghan and Bagh Borj) are located in the SaSZ (Figure 1). The largest garnet deposits are located in the UDMA; several fields lie around Qom-Zanjan, Isfahan, Yazd and Kerman districts (Baghin and Kouh Gabbri).

3.1. Azerbaijan garnet semi-gemstone district

The Azerbaijan district (Figure 1b-Table 1) is the most important garnet semi-gemstone field in northwest Iran.

The deposits of this district are of magmatic, metasomatic and metamorphic origins. As listed in Table 1, the district encompasses seventeen garnet deposits of three main types: 1) Eleven skarns: Pahnavar, Kamtal, Kerenkan, Gowdal, Ayran Goli, Ghinarjeh, Baba Nazar, Agh Daragh, Chopanlar, Anjerd and Zand Abad. Five of these deposits (Pahnavar, Kamtal, Kerenkan, Ghinarjeh, and Baba Nazar) are dominated by grossular-andradite garnets and the rest are dominated by almandine-grossular garnets; 2) two metamorphic amphibolite

deposits: S-Qareaghaj (almandine-spessartine) and Takhte Soleyman (almandine); and 3) two granitoid (magmatic) deposits: Kaleybar (Ti-andradite) and west Qoushchi (almandine) (Hajalioghli *et al.* 2007a; Hajalioghli *et al.* 2007b, 2011; Moazzen and Hajalioghli 2008; Hajalioghli and Moazzen 2009; Ashrafi *et al.* 2009; Moazzen *et al.* 2009; Saki 2010; Mokhtari 2012; Ferdowsi *et al.* 2012, 2015; Sohrabi *et al.* 2015; Asgharzadeh-Asl *et al.* 2017, 2018; Ahangari 2018; Gharesi *et al.* 2018) (Figure 1b). These deposits are located near the Takab, Kaleybar, west Qoushchi and Ahar granitoid intrusions (Hajalioghli *et al.* 2007a; Hajalioghli *et al.* 2007b, 2011; Moazzen and Hajalioghli 2008; Hajalioghli and Moazzen 2009; Ashrafi *et al.* 2009; Moazzen *et al.* 2009; Saki 2010; Mokhtari 2012; Ferdowsi *et al.* 2012, 2015; Sohrabi *et al.* 2015; Advay *et al.* 2017; Asgharzadeh-Asl *et al.* 2017, 2018; Ahangari 2018; Gharesi *et al.* 2018). The Takab complex (related to skarns such as Ghinarjeh, Baba Nazar, Arpachay and garnet amphibolites in S-Qarehaghaj and Takhte Soleyman) experienced regional metamorphism in Precambrian time, overprinted by Paleogene high-grade metamorphism, producing migmatite and granite. Only Takhte Soleyman and W-Qoushchi deposits are part of the SaSZ, the rest are part of the UDMB. The granitoids are small and scattered within the metamorphic rocks. There is no published radiometric age of granitoids, but a Paleogene age is likely (Moazzen and Hajalioghli 2008; Mazhari *et al.* 2009). On the basis of field relations, Lotfi (2001) considered the Takab granitoids to be post-Cretaceous. The intrusive bodies are mainly gabbro, diorite, granite and granodiorite (Figure 2a) (Hajalioghli *et al.* 2011). Chemically, the Takab granitoid rocks are metaluminous and characterized by $ASI < 1.04$ and high contents of CaO (up to 14.5 wt.%), consistent with I-type granitoids (Figure 2b). Low $FeO_{(t)}/(FeO_{(t)}+MgO)$ values (< 0.75) as well as low Nb, Y and K_2O contents show calc-alkaline affinities. Low SiO_2 , K_2O/Na_2O and Al_2O_3 accompanied by high CaO and FeO contents indicate melting of metabasites as an appropriate source for the intrusions. An origin above a subduction zone and crustal melting are inferred for the origin of Takab calc-alkaline intrusions (Figure 3).

The west Qoushchi granite (Figures 1, 2a) contains orthoclase, microcline, plagioclase, muscovite, tourmaline and garnet (Ahangari 2018). Chemical compositions and mineral paragenesis show that the west Qoushchi granite is peraluminous (Figure 2b) and was generated by partial melting of siliciclastic to pelitic rocks. It is an S-type leucogranite (Ahangari 2018) similar to other Early Cretaceous to late Paleocene granites in this district.

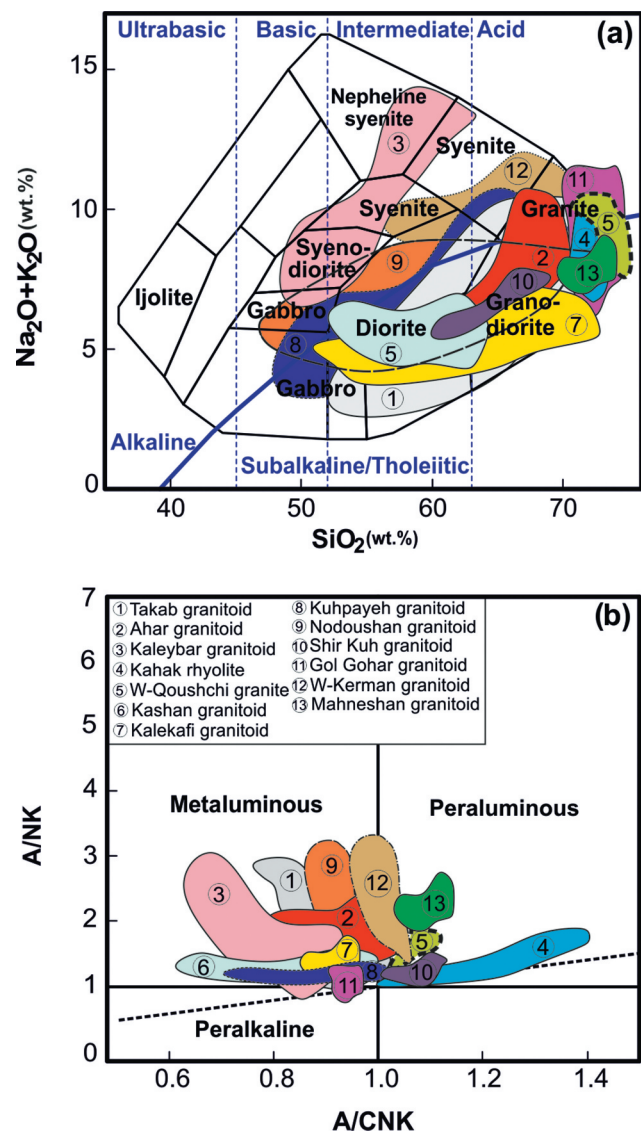


Figure 2. Geochemistry of western Iran granitic rocks. (a) Total alkalis versus SiO_2 diagram (Cox *et al.*, 1979). (b) A/NK (molar $Al_2O_3/(Na_2O+K_2O)$) versus A/CNK (molar $Al_2O_3/(CaO+Na_2O+K_2O)$) diagram (Maniar and Piccoli, 1989). Data for Takab, Ahar, Kaleybar, Kalekafi, Kuhpayeh, Nodoushan, Shir Kuh, Kashan, W-Kerman, Gol Gohar, W-Qoushchi and Kahak felsic rocks (Hajalioghli *et al.*, 2007a, 2007b; Moazzen *et al.*, 2009; Saki, 2010; Hajalioghli *et al.*, 2011; Ahangari, 2018; Mokhtari, 2012; Ferdowsi *et al.*, 2012, 2015; Sohrabi *et al.*, 2015; Advay *et al.*, 2017; Asgharzadeh-Asl *et al.*, 2017, 2018; Gharesi *et al.*, 2018; Ahmadian *et al.*, 2009; Ashrafi *et al.*, 2009; Hajalioghli and Moazzen, 2009, 2011; Sheibi *et al.*, 2010; Saki and Moazzen, 2009; Saki, 2010; Baharifar, 2011; Askari *et al.*, 2015; Mahmoudi and Azadbakht, 2015; Honarmand *et al.*, 2013; Sarjoughian *et al.*, 2018; Amini and Zarei Sahamieh, 2003; Asadollahi *et al.*, 2005; Zarasvandi *et al.*, 2007; Rahgoshay *et al.*, 2008; Zandifar *et al.*, 2008; Ghanei Ardakani and Mackizadeh, 2011; Moore *et al.*, 2012a, 2012b; Taghipour *et al.*, 2013; Zahedi and Boomeri, 2013, 2014, 2016; Mahdizadeh Shahri *et al.*, 2014; Zahedi *et al.*, 2013, 2014; Shafei *et al.*, 2009; Dargahi *et al.*, 2010; Abedpour *et al.*, 2013).

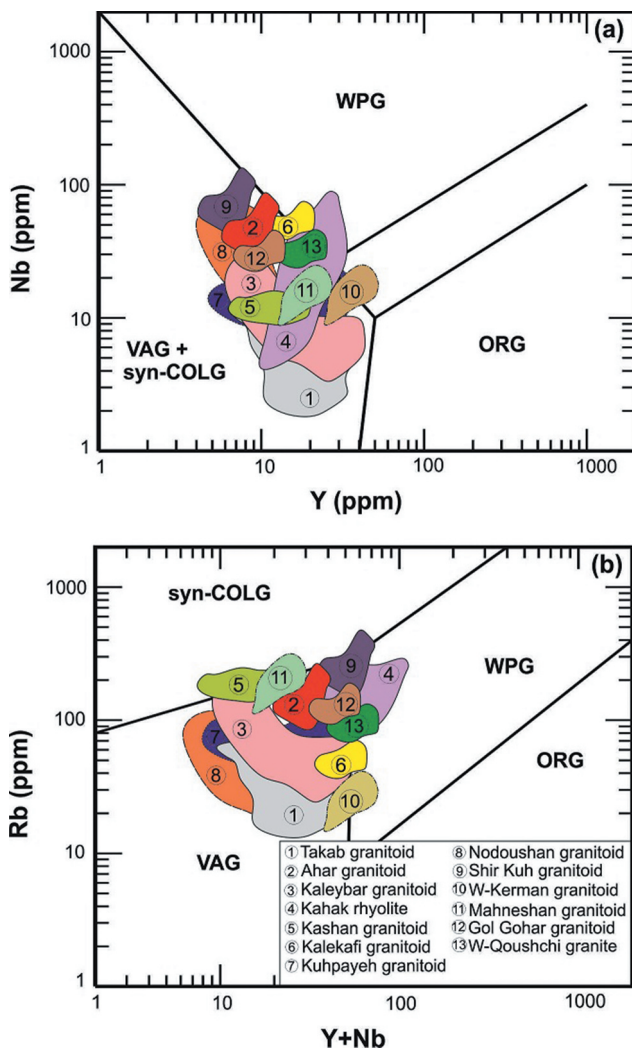


Figure 3. (a, b) Pearce et al. (1984) discriminant diagrams for Takab, Ahar, Kaleybar, Kalekafi, Kuhpayeh, Nodoushan, Shir Kuh, Kashan, W-Kerman, Gol Gohar, W-Qoushchi and Kahak felsic rocks in western Iran. Data for Takab, Ahar, Kaleybar, Kalekafi, Kuhpayeh, Nodoushan, Shir Kuh, Kashan, W-Kerman, Gol Gohar, W-Qoushchi and Kahak felsic rocks from (Hajialioghli et al., 2007a, 2007b; Moazzen et al., 2009; Saki, 2010; Hajialioghli et al., 2011; Ahangari, 2018; Mokhtari, 2012; Ferdowsi et al., 2012, 2015; Sohrabi et al., 2015; Advay et al., 2017; Asgharzadeh-Asl et al., 2017, 2018; Gharesi et al., 2018; Ahmadian et al., 2009; Ashrafi et al., 2009; Hajialioghli and Moazzen, 2009, 2011; Sheibi et al., 2010; Saki and Moazzen, 2009; Saki, 2010; Baharifar, 2011; Askari et al., 2015; Mahmoudi and Azadbakht, 2015; Honarmand et al., 2013; Sarjoughian et al., 2018; Amini and Zarei Sahamieh, 2003; Asadollahi et al., 2005; Zarasvandi et al., 2007; Rahgoshay et al., 2008; Zandifar et al., 2008; Ghanei Ardakani and Mackizadeh, 2011; Moore et al., 2012a, 2012b; Taghipour et al., 2013; Zahedi and Boomeri, 2013, 2014, 2016; Mahdzadeh Shahri et al., 2014; Zahedi et al., 2013, 2014; Shafiei et al., 2009; Dargahi et al., 2010; Abedpour et al., 2013).

The Ahar granitoid (Figure 2a) has moderate to high contents of SiO₂ (56–73 wt.%). It is I-type, sub-alkaline to alkaline and is metaluminous to peraluminous (Figure 1,

2b) (Mokhtari 2012; Ferdowsi et al. 2012, 2015; Sohrabi et al. 2015; Advay et al. 2017; Asgharzadeh-Asl et al. 2017, 2018; Gharesi et al. 2018). In the tectonic discrimination diagram of Pearce et al. (1984), the Ahar granitoid plots within the volcanic arc granite (Figure 3). It has a zircon U-Pb age of 30–23 Ma (Aghazadeh et al. 2011).

The Kaleybar granitoid complex is characterized by low to medium SiO₂ (48–60 wt.%) and medium to high K₂O (2–9 wt.%) (Figure 1, 2). The Kaleybar granitoid contains alkali feldspar, quartz, amphibole, clinopyroxene, biotite and plagioclase (Ashrafi et al. 2009; Hajialioghli and Moazzen 2009; Hajialioghli et al. 2011; Ferdowsi et al. 2015). It is a metaluminous, I-type granitoid (Figure 2b) (Ashrafi et al. 2009; Hajialioghli and Moazzen 2009; Hajialioghli et al. 2011; Ferdowsi et al. 2015). An Eocene-Oligocene age of intrusion can be assigned in view of stratigraphics as well K-Ar and Rb-Sr dating (40–35 Ma; Bagdasaryan and Gukasyan 1962; Gukasyan 1963) from nearby areas in Azerbaijan, significantly older than the Takab and Ahar plutons. The 36 Ma Kaleybar granitoid is shoshonitic and plots in the volcanic arc and within-plate fields due to low Rb (Figure 4) (Ashrafi et al. 2009; Hajialioghli and Moazzen 2009; Hajialioghli et al. 2011; Ferdowsi et al. 2015). Garnets associated with this pluton have magmatic and metamorphic origins.

3.2. Qom-Zanjan garnet semi-gemstone district

The Qom-Zanjan garnet semi-gemstone district (Figure 1b, Table 1) consists of three different types of deposits: 1) almandine garnets around the Boland Parchin metamorphic complex (west Zanjan), andradite-grossular garnets of the Sarvian skarn and almandine garnets of the

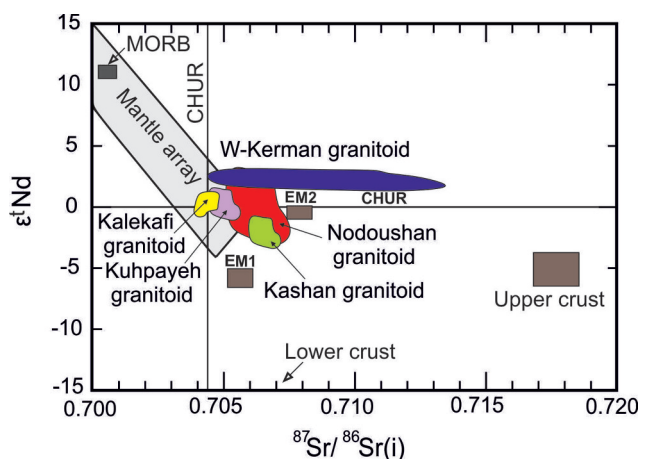


Figure 4. (a) Sr and Nd isotopic data for granitic rocks from Nodoushan, Kashan, Kuhpayeh and W-Kerman granitoids from (Ahmadian et al. 2009; Shafiei et al., 2009; Dargahi et al., 2010; Sarjoughian et al., 2018; Shahsavari et al., 2019).

Table 1. Location of garnet semi-gemstone deposits and their host rocks

Area	Number (Fig.1)	Location	Geology zone	Type of deposit	Chemistry	Form	Colour
Azerbaijan	1	W-Qoushchi	SaSZ	Peraluminous granite	Almandine	Anhedral-subhedral	Brown
	2	NE-Kharvana	UDMA	Skarn	Grossular-andradite	Euhedral-subhedral	Black to grey
	3	Kamtal					
	4	NW-Varzeqan		Alkaline syenite	Ti-andradite	Euhedral-anhedral	Brown, red Light brown, black
	5	Kaleybar					
	6	Ahar		Skarn	Almandine-grossular	Euhedral-subhedral	Black to green
	7	Ayran Goli					
	8	Agh-Daragh					
	9	Chopanlar					
	10	Anjerd					
	11	Zand Abad					
	12	Mazraeh					
	13	NE-Takab			Grossular-andradite	Euhedral-subhedral	Brown, green
	14	Ghinarjeh				Subhedral	
Qom-Zanjan	15	Arpachay		Amphibolite	Almandine	Euhedral	
	16	Takhte Soleyman	SaSZ	Skarn		Euhedral-subhedral	Brown, green, red
	17	Baba Nazar	UDMA		Almandine-spessartine	Euhedral	Dark green
	18	S-Qarehaghaj		Peraluminous granite	Almandine	Euhedral-anhedral	Brown
	19	Boland Parchin	SaSZ	Rhyolite			Red
	20	SE-Qom	UDMA		Andradite-grossular		Green, brown
	21	Qazan		Skarn	Andradite-grossular	Euhedral-subhedral	Dark brown to green
	22	S-Kashan		Skarn		Subhedral-anhedral	Brown
	23	Qohroud				Euhedral	Brown, green
	24	Joveinan				Euhedral-subhedral	Light brown, black
	25	Choogan					
Yazd	26	Kalekafi					
	27	Khumi			Andradite		Green
	28	Fesharak			Andradite-grossular		Green, brown
	29	Vejeh			Andradite		Light brown
	30	Sourk			Andradite		Brown, green
	31	Sadr-Abad					
	32	Khake Sorkh					
	33	Dareh Zereshk		Skarn	Andradite-grossular	Euhedral	Green, brown
	34	Khut			Grossular	Anhedral	Green
	35	Panah Kuh			Andradite	Euhedral-subhedral	Brown, green
Kerman	36	Hosh			Andradite-grossular	Subhedral-anhedral	
	37	Sangestan			Andradite	Euhedral	
	38	Ali Abad			Andradite-grossular	Euhedral-subhedral	Light brown, black
	39	Shir Kuh	SaSZ	Peraluminous granite	Almandine-spessartine		Brown, green
	40	Baghin	UDMA	Skarn	Andradite		
	41	Kouh Gabbri			Andradite-grossular		Yellowish green to dark & emerald green
	42	Bagh Borj			Andradite		
	43	Soghan		Ophiolite			
	44	Gol Gohar	SaSZ	Metamorphic complex	Almandine		Brown, green
	45	Kouh Tanbor			Almandine-grossular-spessartine		Green

References	Host rock	Other mineral	Age(Ma)	Method	Latitude	Longitude
Ahangari (2018) Mokhtari (2012)	Mylonitic gabbro Carbonate and marble	Muscovite, quartz, feldspar, tourmaline Epidote, calcite, pyroxene, chlorite, galena, chalcocopyrite, sphalerite, pyrite, magnetite and amphibole Epidote, calcite, pyroxene, chlorite, galena, chalcocopyrite, sphalerite, pyrite, magnetite and amphibole Garnet, pyroxene, amphibole, quartz, wollastonite, chlorite, epidote, pyrite, pyrothite, malakite, calcite, hematite and magnetite Pyroxene, nepheline, amphibole, feldspar and zeolite Amphibole, Biotite, chlorite, epidote, wollastonite, calcite, quartz, magnetite, hematite, pyrite, gold, calcopyrite, sphalerite and bornite Pyroxene, tremolite, actinolite, epidote, quartz, calcite, magnetite, hematite, calcopyrite, galena and sphalerite	Late Cretaceous to Paleocene 45-20 Ma 45-20 Ma 32-24 Ma 40-35 Ma 32-24 Ma Jurassic 25 Ma 26 Ma 25 Ma 26 Ma 20 Ma 16 Ma Oligo-Miocene 18 Ma 18 Ma 18 Ma 18 Ma 53-43 Ma	Stratigraphy U-Pb K-Ar U-Pb Stratigraphy U-Pb Ar-Ar U-Pb Stratigraphy U-Pb K-Ar	37° 45' 38° 39' 38° 48' 38° 50' 38° 40' 38° 35' 36° 40' 36° 50' 36° 40' 36° 37' 36° 10' 36° 38' 34° 20' 34° 09' 33° 50' 33° 40' 33° 46' 33° 41' 33° 26' 33° 23'	44° 40' 46° 55' 46° 12' 46° 50' 46° 55' 47° 10' 47° 14' 46° 50' 47° 30' 47° 17' 47° 07' 47° 35' 50° 55' 50° 45' 51° 27' 51° 26' 51° 30' 51° 16' 54° 11' 54° 13'
Ferdowsi <i>et al.</i> (2012)						
Abdili <i>et al.</i> (2013)						
Hajjaliloghli and Moazzen (2009) Asgharzadeh Asi <i>et al.</i> (2017) Gharesi <i>et al.</i> (2018)	Nepheline syenite, nepheline diorite and gabbro Granodiorite, quartz monzonite, carbonate and volcanic rocks					
Fallah Karimi (2012)	Schist and marble in neighboring skarn					
Talebi <i>et al.</i> (2016)	Gabbro-granodiorite					
Moazzen and Hajjaliloghli (2008) Alipour <i>et al.</i> (2015)	Amphibolite and schist Hornfels					
Advay <i>et al.</i> (2017) Saki and Moazzen (2009)	Amphibolite Granodiorite, granite and schist					
Baharifar (2011)	Rhyolite					
Zamanian <i>et al.</i> (2017) Chavideh <i>et al.</i> (2018)	Carbonate, marble and granodiorite					
Badr and Hashemi (2016)	Carbonate and marble					
Sherafat (2016)						
Ayati (2017)						
Ranjbar <i>et al.</i> (2016) Ranjbar <i>et al.</i> (2015)	Carbonate, marble and granodiorite					

(Continued)

Table 1. (Continued).

References	Host rock	Other mineral	Age(Ma)	Method	Latitude	Longitude
Ayati (2012)	Carbonate and marble	Calcite, clintonite, spinel, wollastonite and vesuvianite	20 Ma	U-Pb	32° 47'	52°14'
Jamshidzadei et al. (2017)		Calcite, wollastonite, pyroxene and epidote	20 Ma		32° 53'	52°21'
Makizadeh et al. (2007)		Pyroxene, amphibole, calcite and magnetite	31-18 Ma		32° 10'	53°25'
Moshagh et al. (2017)		Olivine, serpentine, pyroxene, talc, flogopite, pyrite, calcopyrite and magnetite	31-18 Ma		31° 45'	543°21'
Maleki et al. (2018)		Pyroxene, amphibole, epidote, calcite, magnetite and serpentine	31-18 Ma		31° 46'	53°21'
Moore et al. (2013)		Pyroxene, epidote, calcite, amphibole, pyrite, magnetite and hematite	16 Ma	K-Ar	31° 33'	53°42'
Zahedi and Boomeri (2013)		Pyroxene, epidote, chlorite, quartz, calcite, pyrite, calcopyrite and hematite	31-16 Ma		31° 52'	53°42'
Zahedi et al. (2013)		Pyroxene, chlorite, epidote, magnetite and calcite	31-16 Ma		31° 54'	53°46'
Rahgoshay et al. (2008)		Pyroxene, feldspar, vesuvianite, pyrite, calcopyrite	31-16 Ma		31° 43'	53°48'
Asadollahi et al. (2006)	Carbonate, conglomerate and marble	Epidote, quartz, calcite and pyrite	31-16 Ma		31° 39'	53°52'
Taghipour et al. (2013)		Epidote, quartz, calcite and pyrite	31-16 Ma		31° 30'	53°38'
Sheibi et al. (2010)	Leucogranite, monzogranite	Biotite, feldspar, quartz, chlorite, prehnite, cordierite and ilmenite	175 Ma	Rb-Sr	31° 30'	54°10'
Malehmir (2016)	Carbonate and marble	Pyroxene, amphibole and calcite	30-6 Ma	U-Pb	30° 56'	56°37'
Abedpour and Tarrah (2010)		Pyroxene, wollastonite, vesuvianite, chlorite, epidote and calcite			30° 23'	56°24'
Montaseri (2011), Dourman and Dirlam (2004)	Ophiolitic complex, gabbro, diorite, serpentinite and asbestiform rocks	Olivine, chlorite, amphibole and serpentine	186-174 Ma	U-Pb	28° 21'	57°47'
Moeinzadeh et al. (2019)	Feldspar, muscovite, quartz, biotite, amphibole, kyanite				28° 19'	57°45'
Moradian et al. (2005), Peighambari et al. (2012)	Biotite, staurolite, chlorite, epidote, muscovite, amphibole and feldspar	Slate, phyllite, schist, amphibolite and granite Phyllite, schist and amphibolite	580 Ma	U-Pb	29° 17'	55°24'
					29° 30'	55°50'

Kahak volcano-sedimentary rocks (southeast Qom) (Figure 1b-Table 1). These deposits are found in two main areas about 50 km apart: Boland Parchin and Sarvian to Kahak (Saki and Moazzen 2009; Saki 2010; Baharifar 2011; Askari *et al.* 2015; Mahmoudi and Azadbakht 2015; Zamanian *et al.* 2017). The deposits are mostly of magmatic and metamorphic origins Table 1. The Mahneshan area is composed of SaSZ metamorphic rocks including amphibolite, meta-ultramafic, gneiss, and granitic gneiss (Hajalioghli *et al.* 2007a; Saki *et al.* 2008), all of which are cut by granitoid intrusions. All rocks are medium to fine-grained and strongly foliated. Field and petrographic observation of these granitoids suggest an association with S-type granite (Hajalioghli *et al.* 2007a; Saki *et al.* 2008). The U-Pb zircon age of granitic gneisses in the Mahneshan complex is 560 Ma (Stockli *et al.* 2004). Apatite U-Th/He (Stockli *et al.* 2004) and Ar-Ar dating of muscovite schist (Gilg *et al.* 2006) constrains the rapid exhumation of Mahneshan basement rocks to the Early Miocene (~20 Ma). The Mahneshan granitic complex is characterized by 69–77 wt.% SiO₂ (Figure 2a), low MgO and very low abundances of high field strength elements (Nb, Ta, Zr and Hf). The Mahneshan granitoid is a peraluminous, S-type granite (Figure 2b) belonging to the medium to high-K alkaline series (Saki and Moazzen 2009; Saki 2010; Mahmoudi and Azadbakht 2015). Saki (2010) proposed that the Mahneshan granitoid was generated in a volcanic arc to syn-collision setting (Figure 3).

Kahak rhyolite outcrops as a crypto-dome and as a dike (Baharifar 2011; Askari *et al.* 2015). Kahak rhyolite was thrust over Late Eocene volcano-sedimentary rocks. These rhyolites have a large range in SiO₂ contents (67–77 wt.%) (Figure 2a). They are S-type and peraluminous granites (Figure 2b). Baharifar (2011) and Askari *et al.* (2015) proposed that the Kahak rhyolitic rocks were generated in post-Eocene time in a volcanic arc to syn-collision tectonic setting (Figure 3).

3.3. Isfahan garnet semi-gemstone district

The Isfahan garnet semi-gemstone district (Figure 1b, Table 1) is located around Kashan, Anarak and Kuhpayeh; the eight deposits in this district are all skarns with metamorphic to metasomatic origins. Seven of these contain andradite-grossular garnet: Qazan, Qohroud, Joveinan, Choogan, Kalekafi, Khuni, and Vejeh. One deposit (Fesharak) is dominated by andradite garnet (Figure 1b, 8, Table 1) (Ayati 2012, 2017; Badr *et al.* 2013; Ashja Ardalan *et al.* 2014; Mohammaddoost *et al.* 2015; Ranjbar *et al.* 2015; Jamshidzaei *et al.* 2017; Chavideh *et al.* 2018).

The Kashan, Kalekafi, and Kuhpayeh intrusions are related to the UDMA. The Kashan pluton (related to the

Qohroud and Joveinan skarns) is dominated by metaluminous diorite (Figure 2b) which crystallized 18 Ma ago (Honarmand *et al.* 2013). The Kashan pluton is coarse to medium grained with medium-K calc alkaline affinities. In the discrimination diagram of Pearce *et al.* (1984), all Kashan granitoids overlap fields of within-plate granite and VAG (Figure 3). Kashan diorites have negative $\epsilon\text{Nd}(t) = -2.6$ to -3.1 and elevated initial $^{87}\text{Sr}/^{86}\text{Sr}$ ratio (0.7066–0.7069), showing evidence for involvement of sediments or older crust (Honarmand *et al.* 2013) (Figure 4).

The Kalekafi granitoid complex (related to the Khuni, Kalekafi and Anarak skarns) (Figure 2a) is mainly metaluminous (Ahmadian *et al.* 2009) (Figure 2b). Kalekafi is an I-type granitoid with high K₂O contents (2.8–5.8 wt.%) (Ahmadian *et al.* 2009). In the tectonic discrimination diagram of Pearce *et al.* (1984) Kalekafi granitoid plots within the VAG, within plate and syn-collisional fields (Figure 3) (Ahmadian *et al.* 2009). It has a whole rock K-Ar age of 53–43 Ma (Perfiliev *et al.* 1979; Jung *et al.* 1985). It has positive $\epsilon\text{Nd}(t)$ values with initial $^{87}\text{Sr}/^{86}\text{Sr}$ in range of 0.7042 to 0.7047 (Figure 4) (Ahmadian *et al.* 2009), differing from the Kashan granitoid.

The Kuhpayeh granitoid complex (related to the Fesharak and Vejeh skarns) consists of voluminous granite, granodiorite, diorite and gabbro (Figure 2a) and ranges widely in SiO₂ contents (46–78 wt.%). Geochemically, the Kuhpayeh granitoid complex is metaluminous to slightly peraluminous and I-type, (Figure 2b) belonging to the calc-alkaline series (Sarjoughian *et al.* 2018). It has initial $^{87}\text{Sr}/^{86}\text{Sr}$ of 0.7053 to 0.7056 and $\epsilon\text{Nd}(t)$ -0.7 to 1.7, consistent with generation by partial melting of crust (Figure 4) (Sarjoughian *et al.* 2018). U-Pb zircon dating indicates an age of 20 Ma for the Kuhpayeh pluton (Sarjoughian and Kananian 2017).

3.4. Yazd garnet semi-gemstone district

The Yazd garnet semi-gemstone district is the most important one in central Iran and consists of 9 skarns and 1 magmatic deposit (Figure 1b, Table 1). Skarns are Khut (grossular), Sourk (andradite), Sadr Abad (andradite), Khake Sorkh (andradite), Dareh Zereskh (andradite-grossular), Ali Abad (andradite-grossular), Panah Kuh (andradite), Sangestan (andradite) and Hosh (andradite-grossular) (Figure 8). These deposits are near the Nodoushan-Taft I-type granitoids (Amini and Zarei Sahamieh 2003; Asadollahi *et al.* 2006; Zarasvandi *et al.* 2007; Rahgoshay *et al.* 2008; Zandifar *et al.* 2008; Ghanei Ardakanei and Mackizadeh 2011; Moore *et al.* 2012b, 2012a; Taghipour *et al.* 2013; Zahedi and Boomeri 2013;

2014; Zahedi and Boomeri 2016; Ghanei Ardakani *et al.* 2014; Zahedi *et al.* 2013; Zahedi *et al.* 2014). Almandine-spessartine garnet in the Shir Kuh S-type granitoid have a magmatic origin (Sheibi *et al.* 2009, 2010); this is related to the SaSZ. The deposits are associated with Late Jurassic to Eocene volcano-sedimentary rocks. The Nodoushan-Taft granitoids are medium to coarse-grained and metaluminous (Figure 3) (Zaravandi *et al.* 2007; Shahsavari *et al.* 2019). Due to their low concentrations of Nb and Ta, the 31–18 Ma Nodoushan-Taft I-type granites (Zaravandi *et al.* 2007; Shahsavari *et al.* 2019) plot in the volcanic arc and syn-collisional granite fields (Figure 3). The $^{87}\text{Sr}/^{86}\text{Sr}(i)$ range from 0.7051 to 0.7080 and $\epsilon_{\text{Nd}}(t)$ values range from -3.2 to +3.8, indicating the involvement of older continental crust and/or sediments (Shahsavari *et al.* 2019). Shir Kuh granitoids differ from Nodoushan-Taft granitoids, because they are generally fine to medium-grained with granodiorite, monzogranite and leucogranite (SiO_2 : 63–76 wt.%) (Figure 2a) (Sheibi *et al.* 2010). Chemical compositions (Sheibi *et al.* 2010) show that the Shir-Kuh granitoid is S-type and peraluminous (Figure 2b) generated by partial melting of metasedimentary rocks. Most Shir Kuh samples plot in the volcanic arc granite field on the Rb versus Y+ Nb diagram, whereas some samples show an affinity with collisional granites (Figure 3) because of their high Rb content (Sheibi *et al.* 2010). U-Pb zircon dating indicates an age of 167–166 Ma for Shir Kuh granitoids (Chiu *et al.* 2013).

3.5. Kerman garnet semi-gemstone district

The Kerman garnet district (Figure 1b, Table 1) is especially important and consists of three principal semi-gemstone areas: west Kerman plutonic complex, Sirjan metamorphic complex and Haji Abad-Esfandagheh ophiolite complexes. Deposits at the three sites have different origins: 1) Skarns including Baghin (andradite) and Kouh Gabbri (andradite-grossular) with metamorphic and metasomatic origin in west of Kerman, 2) related to ophiolite east of Jiroft including Bagh Borj and Soghan with andradite-uvarovite composition and metasomatic origin; 3) SaSZ metamorphic complexes including Kouh Tanbor, Khajoo (almandine-grossular-spessartine) and Gol Gohar (Shang 2010; Abedpour and Tarrah 2010; Montaseri 2011; Abedpour *et al.* 2013; Rahimisadegh *et al.* 2014, 2018; Malehmir 2016; Safarzadeh *et al.* 2016; Fatehi and Ahmadipour 2017; Hosseini *et al.* 2017; Amini and Zolfaghari 2018; Sepidbar *et al.* 2018; Moeinzadeh *et al.* 2019). These deposits are mostly of metamorphic and metasomatic origins Table 1. Soghan and Bagh Borj andradite-

uvarovite garnet is gem-quality green andradite-uvarovite with minor chromium contributing to its valued green color, along with traces of aluminum, titanium, vanadium, and sometimes manganese. Andradite-uvarovite ranges from yellowish or brownish green to 'golden' green, and – the rarest – 'emerald' green.

The Gol Gohar complex consists of Cadomian metamorphic rocks and granitoids (Safarzadeh *et al.* 2016) and low to high grade metavolcanics, marble, schist, amphibolite, gneiss and phyllite. Major and trace element concentrations (e.g. TiO_2 , K_2O and Zr) indicate that the protolith was andesite to rhyodacite. Geochemical discrimination diagrams suggest that amphibolites of the study area formed in a back arc basin tectonic environment, similar to mid-ocean ridge (MORB). The Gol Gohar granitic complex consists of garnet-biotite mylonitic granitoids with high SiO_2 contents (70–74 wt.%). Geochemically, the Gol Gohar granitoid complex is metaluminous and I-type (Figure 2b) belonging to the high K calc-alkaline series. U-Pb zircon dating indicates an age range of 580–538 Ma (Safarzadeh *et al.* 2016).

The west Kerman pluton (Kouh Gabbri) is dominated by granite and alkali granite with metaluminous to rarely peraluminous compositions (Figure 2b) (Shafiei *et al.* 2009; Dargahi *et al.* 2010; Abedpour *et al.* 2013) which intruded Cretaceous to Paleocene limestone and conglomerate. Zircon U-Pb dating by Chiu *et al.* (2013) indicates an age of 30 Ma. The pluton has initial $^{87}\text{Sr}/^{86}\text{Sr}$ of 0.7052–0.7136 and $\epsilon_{\text{Nd}}(t)$ of +2.6 to +3.6. In the discrimination diagram of Pearce *et al.* (1984), all west Kerman granitoids plot close to fields of within plate and VAG (Figure 3) (Shafiei *et al.* 2009; Dargahi *et al.* 2010; Abedpour *et al.* 2013).

Haji Abad-Esfandagheh ophiolites (E-Jiroft area) remnants include Cadomian basement, subduction-related igneous rocks and HP/LT rocks (Moghadam *et al.* 2017). Mantle tectonites constitute the main lithology and are mostly lherzolites and depleted harzburgite with widespread foliated dunite lenses. Podiform chromites are common and typically enveloped by thin dunitic haloes (Moghadam *et al.* 2013). Zircon U-Pb ages from this area provide evidence for Edicaran (547 Ma), Carboniferous (326–312 Ma) and Jurassic (194–186 Ma) magmatic activity (Moghadam *et al.* 2017). Andradite-uvarovite garnet is found within metamorphosed asbestiform gabbro, diorite and serpentinite. Moghadam *et al.* (2017) reported zircon U-Pb ages of 186–174 Ma for the Haji Abad ophiolites. This is significantly older than most Iranian ophiolites, which yield Late Cretaceous ages, and suggest affinities to SaSZ igneous activity.

4. Formation environment of western and southern Iran garnets

Garnet forms in a wide range of environments, from igneous and metamorphic to sedimentary, from the mantle to crust (Baxter *et al.* 2013). Garnet occurs as an important component in the upper mantle. In the crust, garnet is common in metamorphic rocks from greenschist facies to granulites and eclogites. Garnet may form in rocks that are sufficiently rich in trivalent cations Al, Fe³⁺ or Cr and in contact, regional, and subduction related metamorphic rocks. Garnet can also form as a result of anatexis (partial melting of crust or sediments) and happens as an igneous mineral in some S-type and peraluminous granites, resulting from the melting of Al-rich shale (Clemens and Wall 1981). Garnet is also found in the heavy-mineral fraction of sediments and sedimentary rocks. Calcic garnets such as grossular and andradite form in skarn-type contact metamorphic rocks (D'Errico *et al.* 2012; Baxter *et al.* 2013) and in hydrothermal systems (e.g. Méndez-Ortiz *et al.* 2012; Baxter *et al.* 2013).

Garnets in southern and western Iran formed in five main settings: (1) skarn (Asadollahi *et al.* 2006; Rahgoshay *et al.* 2008; Ghanei Ardakani *et al.* 2011; Ferdowsi *et al.* 2012; Moore *et al.*, 2012a; Zahedi and Boomeri 2014 2013; Taghipour *et al.* 2013; Zahedi *et al.* 2014; Ranjbar *et al.* 2015; Sohrabi *et al.* 2015; Alipour *et al.* 2016; Advay *et al.* 2017; Ayati 2017; Jamshidzaei *et al.* 2017; Asgharzadeh-Asl *et al.* 2017, 2018; Chavideh *et al.* 2018; Gharesi *et al.* 2018); (2) peraluminous granitoids and rhyolites (Moradian *et al.* 2005; Saki *et al.* 2010; Sheibi *et al.* 2010; Mahmoudi and Azadbakht 2015; Fatehi and Ahmadipour 2017; Hajjalioghli 2018; Moeinzadeh *et al.* 2019) (3) alkaline rocks (Ashrafi *et al.* 2009; Hajjalioghli and Moazzen 2009; Hajjalioghli *et al.* 2011); (4) metamorphic rocks (Moradian *et al.* 2005; Fatehi and Ahmadipour 2017; Hajjalioghli 2018; Moeinzadeh *et al.* 2019) and (5) related to ophiolites (Douman and Dirlam 2004; Montaseri 2011). These are discussed further as follows:

4.1. Skarn deposits

Skarn deposits (Figure 5a-f) occur as lens where calcareous sediments are intruded by granitic plutons. 35 of the 45 deposits in S- and W- Iran are skarns. Garnet is the main skarn mineral (more than 70% in volume), and is accompanied by calcite, clinopyroxene, actinolite, epidote, quartz, magnetite, hematite, pyrite, and chalcocopyrite (Figure 6a, b). Garnets in hand specimen are chocolate brown to russet in color and related to endoskarn (Einaudi and Burt 1982). Most garnets show atoll texture and have distinct resorbed margins (Figure 6a, b). Sometimes, garnet is replaced by chlorite, amphibole, epidote, calcite and

Fe-oxides (Asadollahi *et al.* 2006; Rahgoshay *et al.* 2008; Ghanei Ardakanei and Mackizadeh 2011; Ferdowsi *et al.* 2012; Moore *et al.* 2012b; Zahedi and Boomeri 2014 2013; Taghipour *et al.* 2013; Zahedi *et al.* 2014; Ranjbar *et al.* 2015; Sohrabi *et al.* 2015; Alipour *et al.* 2016; Advay *et al.* 2017; Ayati 2017; Jamshidzaei *et al.* 2017; Asgharzadeh-Asl *et al.* 2017, 2018; Chavideh *et al.* 2018; Gharesi *et al.* 2018). Clinopyroxene is mainly coarse euhedral to subhedral, has green to dark green color and is included within poikiloblastic garnet. Biotite is replaced by chlorite and amphibole pseudomorphs. Plagioclase is replaced by epidote and calcite.

4.2. Garnet in peraluminous granitoids and rhyolites

Four of the 45 garnet deposits in S and W Iran are in peraluminous felsic rocks. Peraluminous granitoids such as Shir Kuh and Boland Parchin are generally equigranular and fine to coarse grained (Saki 2010; Sheibi *et al.* 2010; Mahmoudi and Azadbakht 2015). The dominant textures are porphyritic granular and cataclastic. The mineralogy generally consists of quartz and K-feldspar and less common plagioclase, garnet, muscovite, biotite cordierite; accessory minerals are ilmenite, zircon, apatite, monazite and sporadic tourmaline (Figure 6c, d). These rocks are regionally deformed and locally have small shear zones. K-feldspar forms most phenocrysts and is common. Quartz is intergrown with K-feldspar and plagioclase in micrographic and myrmekitic texture. Euhedral garnet is the main mafic mineral with or without inclusions such as chlorite. These rocks are regionally deformed with locally developed shear zones (Saki 2010; Sheibi *et al.* 2010; Mahmoudi and Azadbakht 2015). Biotite has a distinctive reddish brown color, locally is altered to chlorite and prehnite and forms elongate lenses parallel to schistosity. Cordierite is euhedral and mostly altered to chlorite (Saki 2010; Sheibi *et al.* 2010; Mahmoudi and Azadbakht 2015). K-feldspar, plagioclase, biotite, garnet and quartz are dominant phases of rhyolites. These minerals occur as small crystals within groundmass and/or as microphenocrysts. K-feldspar and plagioclase show alteration into sericite and clay minerals. Biotite displays brown paleochroism and is fresh with subhedral form. Sometimes plagioclase shows zoning and is altered to clay minerals and sericitic. These rocks are mostly aphyric. The groundmass is altered into clay and chlorite (Baharifar 2011; Askari *et al.* 2015).

4.3. Garnet in alkaline rocks

Only one of the 45 garnet deposits of S and W Iran is found in alkaline rocks. In the Kaleybar region, nepheline syenite contains alkali-feldspar, nepheline, plagioclase, amphibole, clinopyroxene, garnet, biotite and apatite,

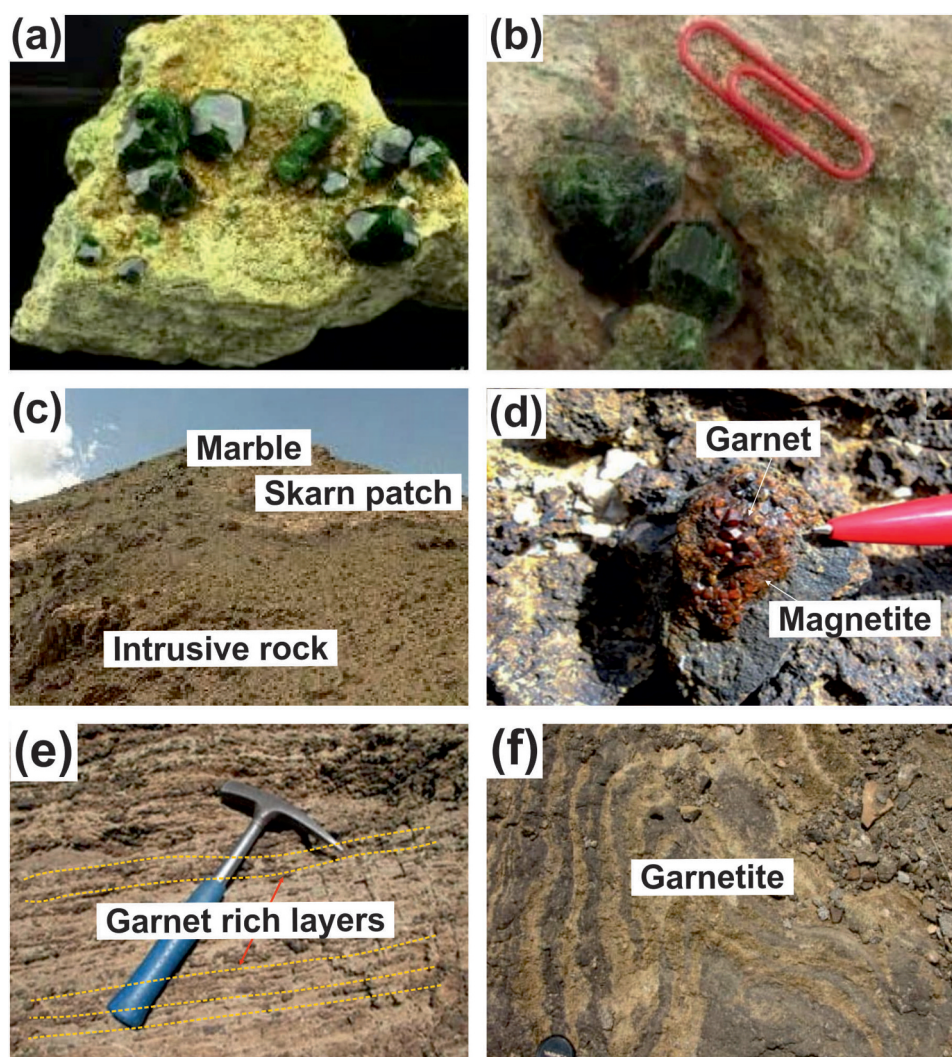


Figure 5. Representative photos of garnetiferous skarns from south and western Iran (a, b) Hand specimen of Baba Nazar garnet (andradite) in skarn from Azerbaijan district (Alipour *et al.*, 2015; Rahimzadeh, 2016). (c) Outcrop of Joveinan garnet (andradite-grossular) in skarn from Isfahan district (Sherafat and Mackizadeh, 2017). (d) Qamsar garnet (andradite-grossular) and magnetite in skarn from Isfahan district (Mohammaddoost *et al.*, 2015). (e) Garnet-rich layers (andradite-grossular) in Vejeh skarn from Isfahan district (Jamshidzai *et al.*, 2017). (f) Joveinan garnetite (andradite-grossular) in skarn from Isfahan district (Sherafat, 2017).

titanite, zircon, spinel, Fe-Ti oxide and quartz minerals. Nepheline is highly pseudomorphed to analcite aggregates (Ashrafi *et al.* 2009; Hajialioghli and Moazzen 2009; Hajialioghli *et al.* 2011). Green to yellow-green Ti-andradite garnets Table 1 is sporadically visible to naked eye within the syenites. One to several crystals, generally with subhedral to euhedral forms, were found in granitoid thin sections, and show equilibrium boundaries with quartz and feldspar.

4.4. Garnet in metamorphic rocks

Three of the 45 garnet deposits in S- and W-Iran are found in schist and amphibolite outcrops around east Takab and and Sirjan areas. These rocks are fine to medium grained and are greenish due to presence of ferromagnesian

minerals or retrograde chlorite alteration from biotite, garnet and hornblende. The rocks have lepidoporphroblastic, porphyroblastic to poikiloblastic textures and contain porphyroblasts of hornblende, biotite, muscovite, chlorite and garnet with quartz inclusions (Figure 6e, f, h). (Table 1). Garnet amphibolites in the E-Takab area are dark grey to black, well foliated and have large garnets. The foliation is accompanied by segregation into dark (hornblende-rich) and light to grey (plagioclase-rich) colored banding (Moradian *et al.* 2005; Fatehi and Ahmadipour 2017; Hajialioghli 2018; Moeinzadeh *et al.* 2019). Petrographically, the amphibolites consist of abundant hornblende, plagioclase, garnet (grossular and almandine-spessartine) and accessory epidote, apatite and opaques. Hornblendes are elongated, parallel to rock foliation. Plagioclase is equant to elongate and,

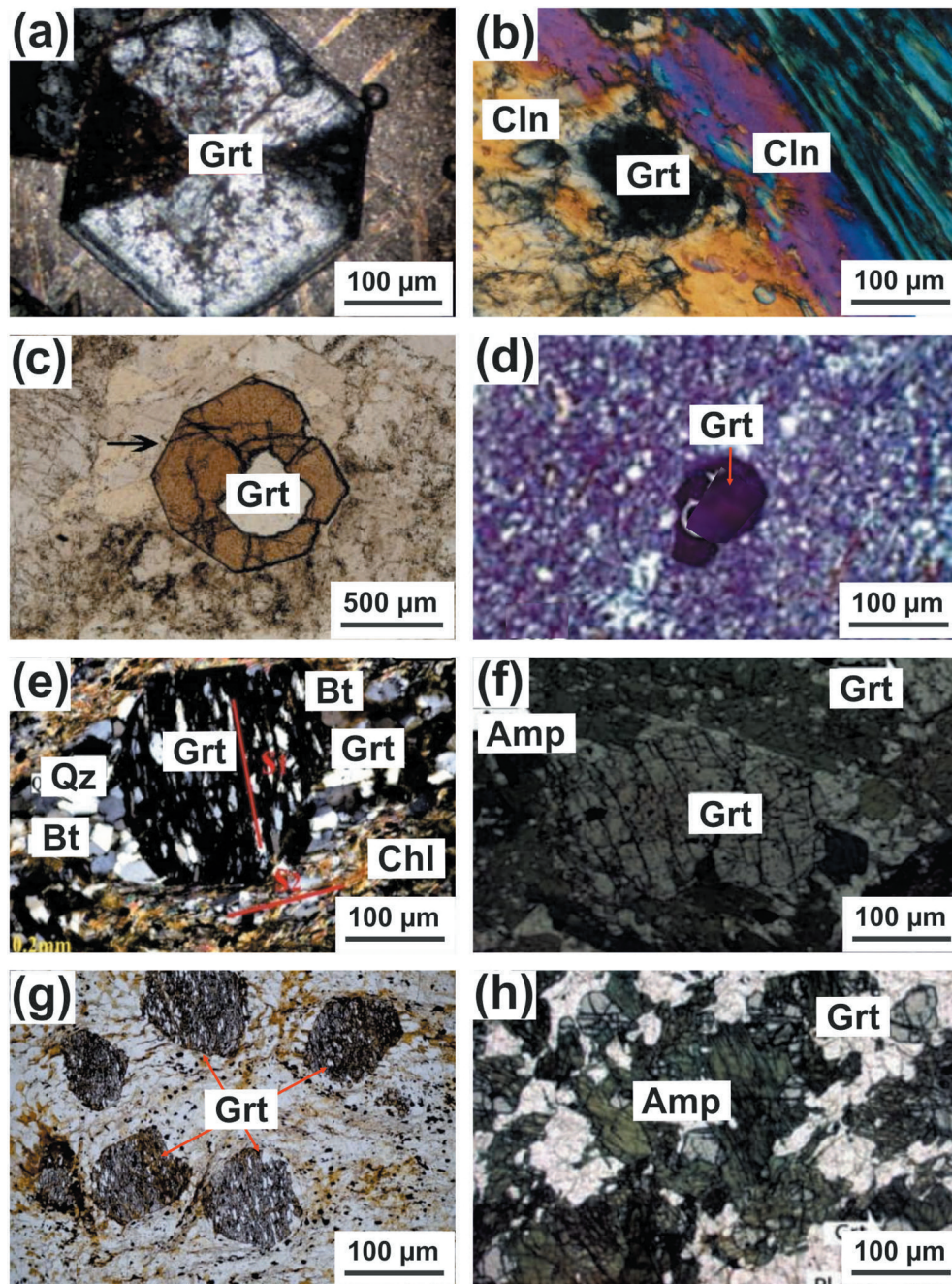


Figure 6. Photomicrographs of garnet (Grt) semi-gemstone in western and southern Iran. (a) Andradite garnet in Khut skarn from Yazd district. (Zahedi et al., 2014). (b) Garnet in clintonnite (Cln) (Ghanei Ardakani and Mackizadeh, 2011) from Yazd district. (c) Atoll almandine garnet texture in peraluminous granite from Qom-Zanjan district (Saki, 2010; Mahmoudi and Azadbakht, 2015). (d) Almandine garnet in Kahak rhyolite from Qom-Zanjan district (Askari et al., 2015). (e) Garnet in schist from Kerman district (Rahimisadegh et al., 2016). (f) Garnet (almandine-spessartine) in amphibolite from Azerbaijan district (Advay et al., 2017). (g) Garnet (almandine) in Bahram Gur schist from Kerman district (Rahimisadegh et al., 2014). (h) Garnet (almandine) in Qarehaghaj amphibolite from Azerbaijan district (Advay et al. 2017). Amp= amphibole, Chr= chromite, Qz= quartz, Cpx= clinopyroxene, Anl= analcite (Whitney and Evans, 2010).

shows twinning due to strain and is partially altered to sericite. Garnet is typically rounded and green to red brown in color and is almandine-spessartine. Garnet cores have numerous inclusions of quartz and plagioclase (Figure 6e, f, h) and some inclusions of magnetite are aligned parallel to foliation.

4.5. Garnet in ophiolites

Two of the 45 garnet deposits of S and W-Iran are found in ophiolites. Deposits of garnet (andradite-uvarovite) (Figure 7g, h, Table 1) are found in the Haji Abad-Esfandagheh ophiolites (Moghadam et al. 2017) of



Figure 7. Representative photos of garnetiferous granitoids, metamorphic rocks, and ophiolites from south and western Iran. (a, b) Ti-rich andradite garnet in Kaleybar granitoid from the Azerbaijan district (Ashrafi et al., 2009). (c) Almandine garnet in Gol Gohar granite from Kerman district (Safarzadeh et al., 2016). (d) Garnet (almandine-spessartine) in Qarehaghaj amphibolite from the Azerbaijan district (Advay et al., 2017). (e, f) Almandine garnet porphyroblasts in Ruchun and Gol Gohar schists from Kerman district (Fatehi and Ahmadipour, 2017). (g, h) Garnets with andradite-grossular and uvarovite in related to ophiolitic complex from the Soghan region in the Kerman district (Montaseri et al., 2013).

Kerman province (Soghan and Bagh Borj). Garnets are found in serpentinized ultramafic rocks mainly consisting of magnetite, pyroxene, and serpentines formed by

metamorphism of mantle rocks. Cr-bearing magnetite is often present. Andradite-uvarovite is found within foliated serpentinites. Garnet colors vary from yellowish

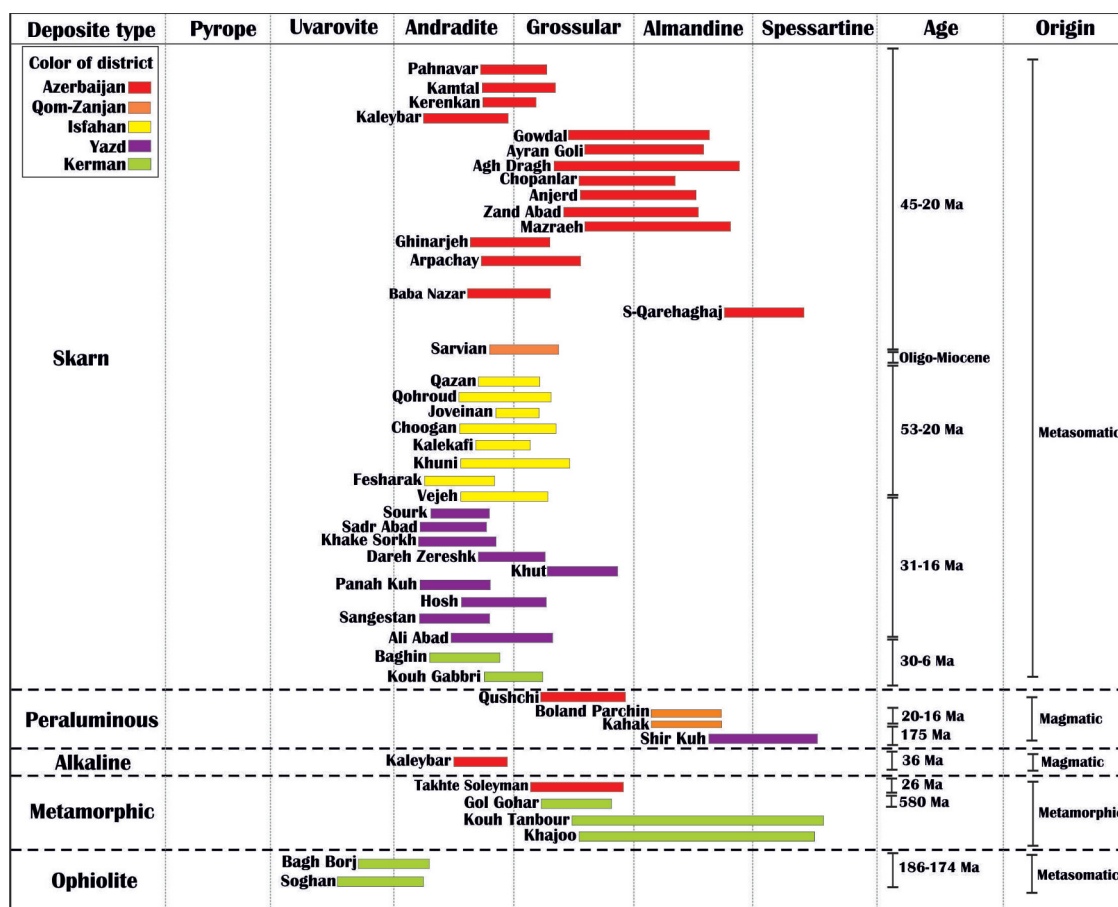


Figure 8. Compositional range of garnets from southern and western Iran. Data for garnets from the Azerbaijan, Qom-Zanjan, Isfahan, Yazd and Kerman districts are from (Hajialioghli et al., 2007a, 2007b, 2011; Hajialioghli and Moazzen, 2009; Moazzen and Hajialioghli, 2008; Ashrafi et al., 2009; Moazzen et al., 2009; Saki and Moazzen, 2009; Saki, 2010; Baharifar, 2011; Mokhtari, 2012; Ferdowsi et al., 2012, 2015; Askari et al., 2015; Mahmoudi and Azadbakht, 2015; Sohrabi et al., 2015; Advay et al., 2017; Asgharzadeh-Asl et al., 2017, 2018; Ahangari, 2018; Gharesi et al., 2018; Badr et al., 2013; Ashja Ardalan et al., 2014; Mohammaddoost et al., 2015; Ranjbar et al., 2015; Ayati, 2012, 2017; Jamshidzai et al., 2017; Chavideh, 2018; Amini and Zarei Sahamieh, 2003; Asadollahi et al., 2005; Zarasvandi et al., 2007; Rahgoshay et al., 2008; Zandifar et al., 2008; Ghanei Ardakani and Mackizadeh, 2011; Moore et al., 2012a, 2013; Taghipour et al., 2013; Zahedi and Boomeri, 2013, 2014, 2016; Ghanei Ardakani et al., 2014; Zahedi et al., 2013, 2014; Abedpour and Tarrah, 2010; Montaseri, 2011; Abedpour et al., 2011, 2013; Malehmir, 2016; Doman and Dirlam, 2004; Mlisenda et al., 2001; Toit et al., 2006; Moradian et al., 2005; Moeinzadeh et al., 2019).

green to bright green. They are generally associated with amphibole, chlorite, apatite and attractively banded layers of apatite and calcite. Some andradite-uvarovite garnets include fibers of chrysotile (horsetail inclusions of serpentine minerals (Dourman and Dirlam 2004; Du Toit et al. 2006; Shang 2010; Abedpour and Tarrah 2010; Montaseri 2011; Malehmir 2016)). This assemblage has hydrothermal origins and formed as a result of retrograde metamorphism (Amthauer and Rossmann 1998).

5. Mineral chemistry

The five types of garnet deposits in S and W Iran are distinguished based on field geology and mineral assemblages as summarized below and on (Figure 8).

5.1. Skarn deposits

Skarn garnets are mostly andradite-grossular but some Azerbaijan deposits are andradite-grossular-almandine and almandine-spessartine (Mokhtari 2012; Ferdowsi et al. 2012, 2015; Sohrabi et al. 2015; Alipour et al. 2015, 2016; Asgharzadeh-Asl et al. 2017, 2018; Talebi et al. 2017; Gharesi et al. 2018). Garnets from Isfahan district skarns (Figure 8) are grossular-andradite. Most have grossular-rich cores with andradite increasing towards the rim (Ayati 2012, 2017; Badr et al. 2013; Ashja Ardalan et al. 2014; Mohammaddoost et al. 2015; Ranjbar et al. 2015; Jamshidzai et al. 2017; Chavideh 2018) (Table, p. 1). Garnets from Yazd district skarns (Figure 8) are predominantly andradite with minor grossular

component (Amini and Zarei Sahamieh 2003; Asadollahi *et al.* 2005; Zarasvandi *et al.* 2007; Rahgoshay *et al.* 2008; Zandifar *et al.* 2008; Ghanei Ardakanei and Mackizadeh 2011; Moore *et al.* 2012b, 2013; Taghipour *et al.* 2013; Zahedi and Boomeri 2013; 2014; Zahedi and Boomeri 2016; Ghanei Ardakani *et al.* 2014; Zahedi and Boomeri 2013; Zahedi *et al.* 2013, 2014). Garnet compositions from Kerman district skarns (Kouh Gabbri, Baghin skarns) are dominantly grossular-andradite and andradite (Abedpour and Tarrah 2010; Abedpour *et al.* 2011; Abedpour *et al.* 2013; Malehmir 2016).

5.2. Garnet in peraluminous granitoids and rhyolites

Garnets in peraluminous granites and rhyolites range from almandine to spessartine. The garnet composition of Boland Parchin granite (Qom-Zanjan district) (Figure 8) is almandine rich (Saki and Moazzen 2009; Saki 2010; Mahmoudi and Azadbakht 2015). In contrast, garnets from the Shir Kuh pluton (Sheibi *et al.* 2009, 2010) contain high almandine-spessartine component Table 1. Garnets from the Qom area (Kahak rhyolite) are predominantly almandine rich (Baharifar 2011; Askari *et al.* 2015), whereas garnets from the west Qoushchi granite are grossular rich (74–79%; Ahangari 2018) Table 1.

5.3. Garnet in alkaline rocks

Garnets from the Kaleybar nepheline syenite are Ti-andradite rich (andradite 67–78%) with TiO₂ content in the range of 1.5–5.0 wt.% (Ashrafi *et al.* 2009; Hajialioghli and Moazzen 2009).

5.4. Garnet in metamorphic rocks

Garnets from metapelites (Kouh Tanbor and Gol Gohar) are grossular and grossular-spessartine (Moradian *et al.* 2005; Moeinzadeh *et al.* 2019). Garnets from Takhte Soleyman amphibolites are grossular (Moazzen and Hajialioghli 2008), in contrast garnets from Khajoo are grossular to spessartine (Moradian *et al.* 2005).

5.5. Garnet in ophiolites

The composition of garnets from Bagh Borj and Soghan are dominantly andradite-uvarovite (Douman and Dirlam 2004; Toit *et al.* 2006; Montaseri 2011).

6. Discussion

6.1. Geological conditions of garnet mineral formation

Below we discuss the geological conditions of garnet mineralization in metamorphic rocks, skarns, peraluminous and alkaline granitoid rocks.

6.1.1. Metamorphic rocks

In metamorphic environments, heat and chemical activity transform the clays of shales and mudstones into minerals such as muscovite, biotite, chlorite and garnet. Under regional metamorphic conditions, garnets form in amphibolite facies ($P < 1.2$ GPa, $T > 500^{\circ}\text{C}$). Clay minerals are potential sources for Al, Mg, Fe and Mn and thus psammopelitic metasediments and carbonates contain sufficient Al, Mg, Fe, Ca, and Mn to produce garnet. Garnets in SaSZ metamorphic rocks probably formed from clay minerals with abundant Fe, Mg, Al and Mn (Figure 11a). During prograde metamorphism, Ca, Al, Mg, Fe and Mn may have been released from the clays and carbonates. Rising temperatures around a cooling pluton results in dehydration metamorphic reactions which will also mobilize Al, Fe, Mg and Mn. Mobilized from sediments, these can mix with magmatic fluids to form garnet.

6.1.2. Peraluminous granitoids

Garnet of peraluminous granitic rocks in the study area show petrographic features similar to magmatic garnets. These are commonly euhedral to subhedral, finely crystalline and mostly free of inclusions (Harrison 1988; Speer and Becker 1992; Whitworth 1992). Magmatic garnets have three modes of occurrence: (1) in strongly peraluminous S-type felsic rocks crystallized under low pressure. For example, thermobarometric studies of garnets from the peraluminous Boland Parchin granite indicate these formed at 486–600°C and 3.2–8 kbar. These garnets tend to be almandine with > 30 wt.% FeO (Clemens and Wall 1984; Lackey *et al.* 2006; Mirnejad *et al.* 2008). (2) in basalts, andesites, dacites, rhyolites or tonalitic and granodioritic porphyries that crystallized under high pressure in the lower crust or mantle. These garnets also tend to be almandine, with 20–30 wt.% FeO, 5–10 wt.% MgO and about 5 wt.% CaO (Day *et al.* 1992; Harangi *et al.* 2001; Aydar and Gourgaude 2002; Yuan *et al.* 2009); and (3) in pegmatites, aplites and granites that crystallized from residual magmatic fluids or highly fractionated magma; these garnets are spessartine that contain up to 30 wt. % MnO (Whitworth 1992). Chemically, peraluminous granite garnet compositions (Miller and Stoddard 1981; Dahlquist *et al.* 2007) plot in the magmatic garnet field which is related to S-type

granites (Figure 9a). This similarity confirms the peraluminous character of the host granite (Figure 9b). S-type felsic rocks are strongly peraluminous ($ASI > 1$) because

they result from partial melting of aluminous metasediments (Figure 11a) (Chapple 1984,1999; Collins and Hobbs 2001; Clemens 2003; Dahlquist *et al.* 2007; Burda

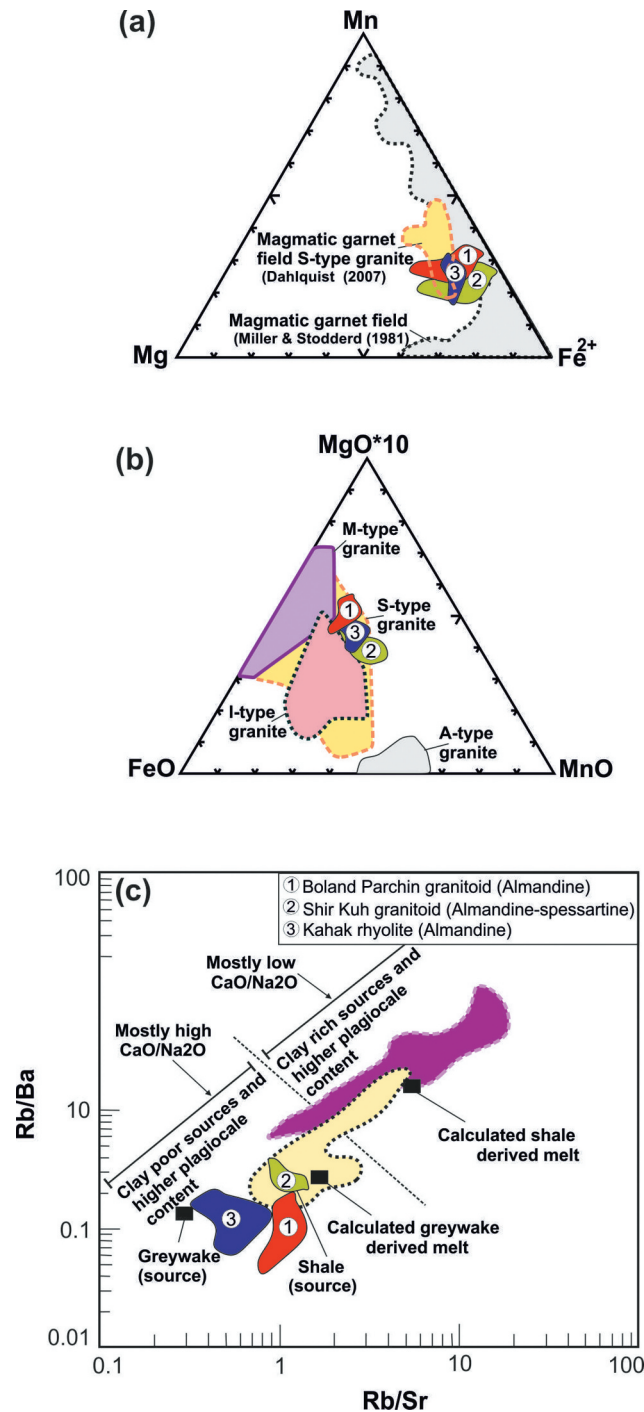


Figure 9. (a) Garnet compositions for western Iran peraluminous granites (Boland Parchin, Shir Kuh) and rhyolite (Kahak) compared with fields for magmatic garnets from Miller and Stoddard (1981) and Dahlquist *et al.* (2007). (b) FeO-MgO-MnO ternary diagram of garnets from various granites. Data for garnet in I-type granites from Wu *et al.* (2004) and Yu *et al.* (2004); S-type granites from Plank (1987), Kebede *et al.* (2001), Jung *et al.* (2001), Jung and Hellebrand (2006), and Dahlquist *et al.* (2007); A-type granites, Bray (1988), Wu *et al.* (2004), Wang *et al.* (2003), Zhang *et al.* (2012) igneous rocks originating from the mantle, Chen and Zhao (1991), Harangi *et al.* (2001), Kawabata and Takafuji (2005). (c) Rb/Sr versus Rb/Ba diagram for determining sources of peraluminous granites, fields from Sylvester (1998). Fields for Kahak rhyolite, Boland Parchin and Shir Kuh granite are from (Saki and Moazzen, 2009; Sheibi *et al.*, 2009; Sheibi and Esmaily, 2010; Baharifar, 2011).

et al. 2009). Partial melts of metasediments produce leucogranite with FeO+MgO contents below 4 wt.% (Montel and Vielzeuf 1997).

Some researchers believe that S-type granite are products of incongruent fluid-absent melting of biotite in aluminous sources. Clemens (1992) and Patino-Douce and Beard (1996) demonstrated that melts produced via the anatexis of metapelites and metagreywackes (Figure 11b) are limited to leucogranite compositions, particularly if it is considered that temperatures within the crust rarely exceed 900°C (Harley 1998). The existence of garnet and muscovite reflect the strongly peraluminous nature of the studied granites and confirms an aluminous metasedimentary source. The low content of Fe and Mg in S-type granites show that the anatectic temperatures were mostly below the biotite solidus or that the source rocks contained little biotite. The partial melting of metagreywacke and metapelite source rocks is also demonstrated by plotting the studied leucogranites in the fields of experimental melts derived from partial melting of different sources (Figure 9c). The chemical composition of garnets and whole rock hosts show that the garnets could have formed by crystallization from the peraluminous magma in equilibrium with solid phases such as biotite.

6.1.3. Alkaline igneous rocks

Ti-bearing garnets form in a variety of alkaline igneous rocks (Huggins et al. 1977a, 1977b; Dingwell et al. 1985), chiefly in strongly silica under-saturated rocks (Figure 11c). These garnets contain Ti, a quadrivalent cation not generally found in garnets (Dingwell and Brearley 1985). In some Kaleybar syenite samples, garnet compositions projected onto the spessartine+pyrope-Ti-andradite-grossular system lie in the Ti-rich andradite field (Figure 13) (Deer et al. 1982; Dingwell and Brearley 1985). Ti-rich andradite garnets can be further categorized into melanite and schorlomite, depending on whether Fe³⁺ or Ti prevails in the octahedral site. The studied Ti-andradites from the Kaleybar alkaline complex plot as Ti-andradite and melanite (Deer et al. 1992; Dawson et al. 1995; Gwalani and Rock 2000). When Kaleybar garnet compositions are plotted on the TiO₂ (wt.%) versus Fe₂O₃ (wt.%) diagram (Figure 10) (Brod 2003), all plot below the 5 wt.% TiO₂ line and occupy the field of Ti-andradite (Figure 10). Kaleybar garnet TiO₂ versus Fe₂O₃ plot suggests similarities to those of alkaline igneous rocks from Alberta, Canada (Saha et al. 2011).

Ti-bearing andradite garnets (Howie and Woolley 1968; Lang et al. 1995; Russell et al. 1999) can crystallize both in magmatic and hydrothermal environments

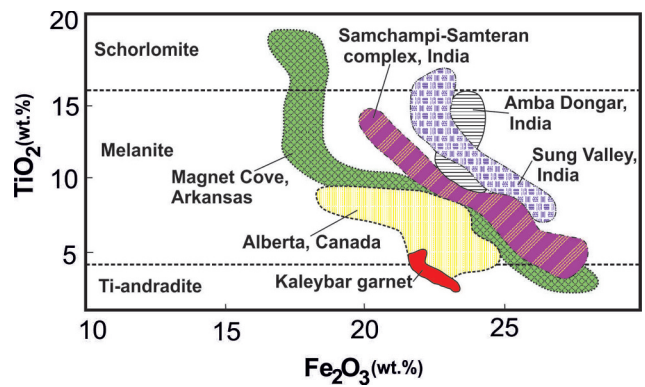


Figure 10. TiO₂ versus Fe₂O₃ diagram showing the fields of schorlomite, melanite and Ti-andradite (Saha et al. 2011). The compositional range of garnets from Kaleybar nepheline syenite falls in the Ti-andradite field. Compositional fields of garnets from other alkaline complexes are also shown. Field for Kaleybar alkaline granite and garnet are from Hajjaliooghi and Moazzen (2009) and Ashrafi et al. (2009).

(Jamtveit and Hervig 1994). Most Ti-rich andradite forms in silica under-saturated alkaline igneous rocks as primary garnet (Figure 11c) (e.g. Huggins et al. 1977a, 1977b; Deer et al. 1982; Meagher 1982). Secondary type occurs usually in skarns, veins and metasomatic rocks and have lower TiO₂ contents (Howie and Wolley 1968; Manning and Harris 1970; Deer et al. 1982). Ti-garnet types are distinguished on the basis of color, morphology, zonation style, and major oxides criteria (Cioni et al. 1995; Russell et al. 1999; Naimo et al. 2003; Smith et al. 2004; Fulignati et al. 2004). Magmatic Ti-garnet in alkaline rocks such as syenite and nepheline syenite are dark brown or black in color (Turbeville 1993; Lang et al. 1995). This is due to the abundance of titanium (>1 wt.%) (Scheibner et al. 2007). In contrast, Ti-garnet produced by metasomatism or hydrothermal activity are red, yellow, brown and green because of their low TiO₂ contents. Euhedral garnet is a strong indicator of primary (magmatic) origin, while interstitial or irregular grains reveal complex metasomatic or hydrothermal formation due to reactions of earlier mafic minerals with late stage fluids (Figure 11c). Armbruster et al. (1998) proposed an association between petrogenesis and Ti-substitutions in these minerals. Garnet crystals with schorlomite substitution (Ti⁴⁺→Si⁴⁺) are of magmatic origin, whereas crystals with combined morimotoite (Fe²⁺+Ti⁴⁺→2Fe³⁺) and hydro-garnet substitutions (O₄H₄→SiO₄) often form as a result of metamorphism (Armbruster et al. 1998). Garnets in skarns exhibit a mixture between morimotoite and schorlomite substitutions (Armbruster et al. 1998). Ti-rich garnet in skarns can be produced by the breakdown of titanian-bearing phases such as titanite and ilmenite under oxidizing conditions and low SiO₂ in the melt or in the hydrothermal fluid (Russell et al. 1999). The

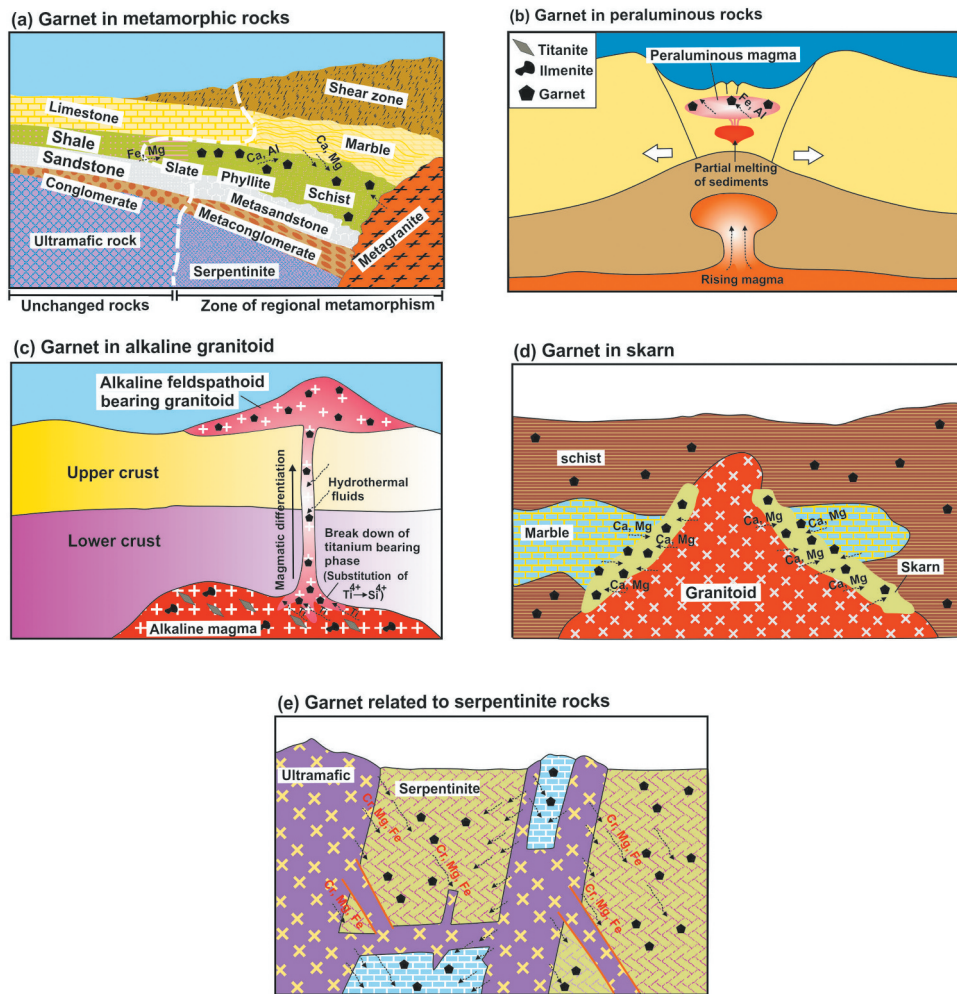


Figure 11. Schematic model presenting the various environments related to crystallization of Iran garnets in (a) metamorphic rocks, (b) peraluminous rocks, (c) alkaline granitoids, (d) skarn and (e) related to ophiolite. See text for further explanation.

Ti-rich garnets of the Kaleybar alkaline rocks likely formed from silica-undersaturated magmas (Nash 1972; Woolley 1973; Gwalani *et al.* 2000).

6.1.4. Skarns

Skarns form where limestones (with more CO₂, Ca, and sometimes Mg) interact with hot hydrous fluids from intrusive rocks (with more Fe, K, Na and Si). These fluids transform host rocks surrounding intrusive contacts into skarns. Calc-silicate rocks of skarns show a variety of textures, compositions and origins (Einaudi and Burt 1982). Skarns can be classified according to the rock type replaced (Einaudi and Burt 1982), including exoskarn and endoskarn which describe replacements of carbonates and intrusive rocks, respectively. Endoskarn is found where metasomatic fluids exploited highly fractured intrusions and along the contact with shale and limestone as conduits (Einaudi and Burt 1982). No endoskarns are documented among the 35 skarns in our compilation, they

are all exoskarns. Magnesian exoskarns are dominated by Mg-silicates such as forsterite or its alteration product serpentine, usually along with diopside, calcite and spinel (Einaudi and Burt 1982). In contrast, garnet (grossular-andradite) and pyroxene are the dominant minerals in calcic exoskarns. All skarns in the study area are exoskarns that occur as lenses in marble and/or adjacent portion of the marble and/or along the contact between the marble and intrusive bodies. In western and southern Iran skarns the main minerals are epidote, grossular-andradite, diopside and calcite with less quartz and amphibole, although grossular-almandine is abundant in Azerbaijan skarns.

Two stages of alteration are expected in skarn systems: prograde and retrograde. During the metasomatic prograde stage ($T > \sim 750^{\circ}\text{C}$), anhydrous calcium silicate minerals garnet (andradite-grossular) and clinopyroxene form. During retrogression ($T < \sim 750^{\circ}\text{C}$), other minerals such as epidote, hornblende, calcite, quartz and chlorite may form (Amini and Zarei Sahamieh 2003; Moazzen

et al. 2009; Ghanei Ardakane and Mackizadeh 2011; Mokhtari 2012; Ferdowsi *et al.* 2012, 2015; Badr *et al.* 2013; Zahedi *et al.* 2013; Zahedi *et al.* 2014; Sohrabi *et al.* 2015; Asgharzadeh-Asl *et al.* 2017, 2018; Ahangari 2018; Gharesi *et al.* 2018; Ashja Ardalan *et al.* 2014; Ranjbar *et al.* 2015; Ayati 2017; Jamshidzai *et al.* 2017; Chavideh *et al.* 2018). At still lower T, the assemblage of hydrous and anhydrous calcium silicate minerals can recrystallize into finer-grained assemblages of chlorite, calcite, quartz and clay. During the metasomatic prograde stage (Figure 11d) the addition of Fe and Si via the magmatic fluid (Pirajno 2013) into carbonate rocks makes new calc-silicate minerals, such as clinopyroxene and garnet (Figure 11d). Ugrandite (uvarovite-andradite-grossular) garnet makes up most skarns (Amini and Zarei Sahamieh 2003; Asadollahi *et al.* 2005; Zarasvandi *et al.* 2007; Rahgoshay *et al.* 2008; Zandifar *et al.* 2008; Hajialioghli and Moazzen 2009; Moazzen *et al.* 2009; Mokhtari 2012; Ferdowsi *et al.* 2012, 2015; Badr *et al.* 2013; Zahedi *et al.* 2013, 2014; Sohrabi *et al.* 2015; Asgharzadeh-Asl *et al.* 2017, 2018; Ahangari 2018; Gharesi *et al.* 2018; Ashja Ardalan *et al.* 2014; Mohammaddoost *et al.* 2015; Ranjbar *et al.* 2015; Ayati 2012, 2017; Jamshidzai *et al.* 2017; Chavideh *et al.* 2018). Intrusive bodies are the source of silica-rich hydrous fluids in most skarns. During prograde metamorphism of sedimentary rocks, decarbonation and dehydration reactions yield CO₂ and H₂O, some of which concentrate at lithologic boundaries (Cartwright 1994). These metamorphic fluids dissolve some components of the primary rock and can transport these to sites of skarn formation (Figure 11d). As shown in (Figure 11), formation of skarns in the region can be attributed to the interaction of the masses and host rocks as a result of Jurassic and Paleogene intrusions. These skarn rocks are dominated by garnet minerals, clinopyroxene and plagioclase along with epidote which may be as a result of retrograde metamorphism.

6.1.5. Ophiolitic garnets

Chromium-bearing garnets are uncommon and related to unusual geological and geochemical environments. In the Kerman district, Haji Abad-Esfandagheh ophiolites in the E-Jiroft area include mantle tectonites as the main lithology. These are mostly lherzolites and depleted harzburgites with widespread foliated dunite lenses. Podiform chromites are common and are typically enveloped by thin dunitic haloes (Moghadam *et al.* 2013). Some of the garnets in serpentinized peridotite are rich in chromium, suggesting some mobility of chromiferous solutions during formation (Figure 11e; Douman and Dirlam 2004; Mayerson *et al.* 2006; Shang 2010; Montaseri 2011). Chromium was released from the

serpentinized peridotites (Figure 11e) in a Fe-rich and Al poor environment. In such a situation late stage hydrothermal metasomatism advanced along the cracks of serpentine, causing in the precipitation of demantoid garnet in serpentinite veins (Štubňa *et al.* 2019).

8. Conclusions

The following conclusions result from this study:

- A garnet semi-gemstone province in southern and western Iran is recognized and subdivided into five districts: Azerbaijan, Qom-Zanjan, Isfahan, Yazd and Kerman. Garnet deposits encompass the Sanandj-Sirjan Zone and Urumieh-Dokhtar magmatic assemblage.
- 45 deposits are identified. Garnets are concentrated in a variety of rocks including (1) skarn; (2) peraluminous granitoids and rhyolites; (3) alkaline granite; (4) metamorphic rocks; and (5) related to ophiolitic complex. Most (78%) of these deposits are skarns.
- Garnets are mostly grossular-andradite in skarn, Ti-andradite in alkaline granite, almandine in peraluminous granite and volcanic rocks, almandine-grossular-spessartine in metamorphic rocks and andradite-grossular and uvarovite in ophiolitic complex.
- Fluids responsible for garnet mineralization in skarns, metamorphic rocks and ophiolites were exsolved from cooling granitic bodies and released by metamorphosed sediments. Transformation of clinopyroxene in syenite rocks due to alkaline metasomatic reactions between earlier formed mafic mineral and late stage fluids and formed Ti-rich garnet.
- Garnet grew in magma in peraluminous igneous rocks.

Highlights

- Garnets are widespread accessory minerals in igneous and metamorphic rocks of western and southern Iran.
- Garnet deposits of western and southern Iran show six associations: (1) skarn; (2) peraluminous granitoid and rhyolite; (3) alkaline granite; (4) metamorphic rocks; and (5) ophiolites.
- Garnets are mostly related to skarns around Cenozoic granitoid intrusions.
- Fluids responsible for garnet mineralization in skarns, metamorphic rocks and ophiolites were exsolved from cooling granitic bodies and released by metamorphosed sediments.

Acknowledgments

We thank A.A. Baharifar, Hajialioghli, R., Moazzen, M., Ashrafi, N., Saki, A., Mokhtari, M.A.A, Ferdowsi, R., Sohrabi, G., Asgharzadeh-

Asl, H., Ahangari, M., Gharezi, A., Askari, N., Mahmoudi, S., Baharifar, A., Ayati, F., Ranjbar, S., Jamshidzaei, A., Chavideh, M., Badr, A., Ashja Ardralan, A., Moahammaddoust, H., Zarasvandi, A., Zandifar, S., Ghanei Ardakani, J., Taghipour, B., Montaseri, M., Abedpour, Z., Rahimisadegh, H., Safarzadeh, M., Sherafat, S., Peighambari, S., Zahedi, A., for sharing photos and chemical data used in this paper. This is UTD Geosciences contribution number 1336. . This version benefitted much from the critical comments of Dr. H. Shafaii Moghadam, editor and anonymous reviewer and F. Sepidbar.

Disclosure statement

No potential conflict of interest was reported by the authors

ORCID

Hossein Azizi  <http://orcid.org/0000-0001-5686-4340>

References

- Abdili, M., Moayyed, M., Jahangiri, A., and Hosseinzadeh, G., 2013, Study of relationship between intrusion body and skarn in Kerenkan (East Azerbaijan, NW of Varzeghan): First Iranian conference on Applied Geology, Damghan, Iran.
- Abedpour, Z., Mir Hosseini, S.M., Ahmadi Pour, H., and Ghasemi, H., 2013, Petrography, geochemistry and tectonic setting of the Kuh Gabbri granitoid, Rafsanjan: Iranian Journal of Geology, v. 27, p. 75–87. (*in Persian*).
- Abedpour, Z., and Tarrah, J., 2010, Petrography and Mineralogical reactions relating skarn zones at the Kuh-eGabbri, Northwestern Kerman: The 1st International Applied Geological Congress, Department of Geology, Islamic Azad University-Mashhad Branch, Mashhad, Iran, 26–28.
- Advay, M., Hajialioghli, R., and Moazzen, M., 2017, Mineral chemistry and P-T estimations of Grt-Cpx amphibolites, South of Qarehaghaj-east Azerbaijan province: Scientific Quarterly Journal, Geosciences, v. 526, p. 29–42. (*in Persian*). doi:10.22071/gsj.2016.5016.
- Agard, P., Omrani, J., Jolivet, L., and Mouthereau, F., 2005, Convergence history across Zagros (Iran): Constraints from collisional and earlier deformation: International Journal of Earth Sciences, v. 94, no. 3, p. 401–419. doi:10.1007/s00531-005-0481-4.
- Agard, P., Omrani, J., Jolivet, L., Whitechurch, H., Vrielynck, B., Spakman, W., Monié, P., Meyer, B., and Wortel, R., 2011, Zagros orogeny: A subduction-dominated process: Geological Magazine, v. 148, no. 5–6, p. 692–725. doi:10.1017/S001675681100046X.
- Aghazadeh, M., Castro, A., Badrzadeh, Z., and Vogt, K., 2011, Post-collisional polycyclic plutonism from the Zagros hinterland: The Shaivar Dagh plutonic complex, Alborz belt, Iran: Geological Magazine, v. 148, no. 5–6, p. 980–1008. doi:10.1017/S0016756811000380.
- Aghazadeh, M., Castro, A., Omran, N.R., Emami, M.H., Moinvaziri, H., and Badrzadeh, Z., 2010, The gabbro (shoshonitic)–monzonite–granodiorite association of Khankandi pluton, Alborz Mountains, NW Iran: Journal of Asian Earth Sciences, v. 38, no. 5, p. 199–219. doi:10.1016/j.jseas.2010.01.002.
- Ahangari, M., 2018, Origin of tourmaline and garnet in west Qushchi mylonite granite (NW Iran); constrains on petrogenesis of parental rock. Iran: Iranian Journal of Crystallography and Mineralogy, v. 25, no. 4, p. 697–710. (*in Persian*). doi:10.29252/ijcm.25.4.697.
- Ahmadian, J., Haschke, M., Mcdonald, I., Regelous, M., Ghorbani, M.R., Emami, M.H., and Murata, M., 2009, High magmatic flux during Alpine-Himalayan collision: Constraints from the Kal-e-Kafi complex, central Iran: Geological Society of American Bulletin, v. 121, no. 5–6, p. 857–868. doi:10.1130/B26279.1.
- Alavi, M., 1994, Tectonics of the Zagros orogenic belt of Iran: New data and interpretations: Tectonophysics, v. 229, no. 3–4, p. 211–238. doi:10.1016/0040-1951(94)90030-2.
- Alavi, M., 2007, Structures of the Zagros fold-thrust belt in Iran: American Journal of Science, v. 307, no. 9, p. 1064–1095. doi:10.2475/09.2007.02.
- Alipour, S., Shirmohammadi, P., and Rahim Souri, Y., 2015, Geochemistry of REEs and reconstruction of structural formula of Baba-Nazar garnet index, Takab, W. Azarbayedjan, Iran: Petrology, v. 23, p. 83–96. (*in Persian*).
- Alipour, S., Shirmohammadi, P., Rahimsouri, Y., and Bagheri, H., 2016, Geochemistry, petrography and fluid inclusion studies of Baba Nazar garnet index, Takab, west Azarbaijan province: Scientific Quarterly Journal, Geosciences, v. 25, p. 349–362. (*in Persian*). doi:10.22071/gsj.2016.41234.
- Amini, M., and Zolfaghari, A., 2018, Investigating the potentials of gemstones in the Kuh- Gabri Skarn, Kerman Province: 25th Symposium of Crystallography and Mineralogy of Iran, Yazd University, Yazd.
- Amini, S., and Zarei Sahamieh, R., 2003, Mineralogical and Geochemical characteristics of “Khezr-Abad pluton” NW of Taft, Iran. Iran: Iranian Journal of Crystallography and Mineralogy, v. 11, p. 83–100. (*in Persian*).
- Amthauer, G., and Rossman, G.R., 1998, The hydrous component in andradite garnet: European Journal of Mineralogy, v. 83, p. 835–840.
- Armbruster, T., Birrer, J., Libowitzky, E., and Beran, A., 1998, Crystal chemistry of Ti-bearing andradites: European Journal of Mineralogy, v. 10, no. 5, p. 907–921. doi:10.1127/ejm/10/5/0907
- Asadollahi, P., Khalili, M., and Makizadeh, M.A., 2006, Garnet genesis in altered conglomerate of Sangestan Formation, Damak Aliabad (west of Taft), Yazd Province: Iranian Journal of Geosciences, v. 2, p. 263–273. (*in Persian*).
- Asgharzadeh-Asl, H., Tale Fazel, E., and Mehrabi, B., 2017, Mineralogy, occurrence of mineralization and temperature-pressure conditions of the Agh-Daragh polymetallic deposit in the Ahar-Arasbaran metallogenic area: Economic Geology, v. 9, p. 1–23. (*in Persian*). doi:10.22067/econg.v9i1.44244.
- Asgharzadeh-Asl, H., Tale Fazel, E., Mehrabi, B., and Masoudi, F., 2018, Geochemical-metallogenic evolution of Agh-Daragh igneous rocks (north of Ahar) links to Cu-Au±W occurrences: Petrology, v. 38, p. 21–44. (*in Persian*). doi:10.22108/ijp.2017.100426.0.
- Ashja Ardalan, A., Khodadadi, M., Emami, M.H., Sheikh Zakariaie, J., Razavi, M.H., and Yazdi, A.A., 2014, Geochemistry and Petrogenesis of granitoid pluton and enclaves in Qohroud-Kashan: Indian Journal of Fundamental and Applied Life Sciences, v. 14, p. 1693–1709.

- Ashrafi, N., Ameri, A., Jahangiri, A., Hasebe, N., and Eby, G.N., 2009, Mineral chemistry of garnets in the Kaleybar alkaline igneous intrusion, NW Iran: *Iranian Journal of Crystallography and Mineralogy*, v. 17, p. 357–368. (*in Persian*).
- Askari, A., Karimpour, M.H., Mazaheri, S.A., and Malekzadeh, A., 2015, Petrography, geochemistry and origin of garnet-bearing rhyolites of Kahak area, SE Qom, Iran: *Scientific Quarterly Journal, Geosciences*, v. 94, p. 17–26. (*in Persian*). doi:10.22071/gsj.2014.53661.
- Ayati, F., 2012, Studies of metamorphic zones and the study of garnet chemistry in the Mazraeh Hana skarns: Research papers of Payame Noor University of Chaharmahal and Bakhtiari Province, Basic Special Issue of Science and Engineering, 5
- Ayati, F., 2017, Mineralogy and origin of iron-rich garnetites in the Choogan area-North of Meime: *Scientific Quarterly Journal, Geosciences*, v. 27, p. 3–12. (*in Persian*). doi:10.22071/gsj.2017.54125.
- Aydar, E., and Gourgaud, A., 2002, Garnet-bearing basalts: An example from MtHasan, Central Anatolia, Turkey: *Mineralogy and Petrology*, v. 75, p. 185–201. doi:10.1093/petrology/33.1.125.
- Azizi, H., and Asahara, Y., 2013, Juvenile granite in the Sanandaj–Sirjan Zone, NW Iran: Late Jurassic–early Cretaceous arc–continent collision: *International Geology Review*, v. 55, no. 12, p. 1523–1540. doi:10.1080/00206814.2013.782959.
- Azizi, H., Asahara, Y., Mehrabi, B., and Chung, S.L., 2011, Geochronological and geochemical constraints on the petrogenesis of high-K granite from the Suffi abad area, Sanandaj–Sirjan Zone, NW Iran: *Chemie Der Erde-Geochemistry*, v. 71, no. 4, p. 363–376. doi:10.1016/j.chemer.2011.06.005.
- Azizi, H., and Moinevaziri, H., 2009, Review of the tectonic setting of Cretaceous to Quaternary volcanism in northwestern Iran: *Journal of Geodynamics*, v. 47, no. 4, p. 167–179. doi:10.1016/j.jog.2008.12.002.
- Azizi, H., and Stern, R.J., 2019, Jurassic igneous rocks of the central Sanandaj–Sirjan zone (Iran) mark a propagating continental rift, not a magmatic arc: *Terra Nova*, v. 31, p. 415–423.
- Azizi, H., Zanjefili-Beiranvand, M., and Asahara, Y., 2015, Zircon U–Pb ages and petrogenesis of a tonalite–trondhjemite–granodiorite (TTG) complex in the northern Sanandaj–Sirjan zone, northwest Iran: Evidence for Late Jurassic arc–continent collision: *Lithos*, v. 216, p. 178–195.
- Badr, A., Davoudian, A.R., Shabani, N., Azizi, H., Asahara, Y., Neubauer, F., Dong, Y., and Yamamoto, K., 2018, A- and I-type metagranites from the North Shahrekord Metamorphic Complex, Iran: Evidence for Early Paleozoic post-collisional magmatism: *Lithos*, v. 300, p. 86–104. doi:10.1016/j.lithos.2017.12.008.
- Badr, A., and Hashemi, M., 2016, Jewellery garnets in skarn east of Ghahrood (Isfahan Province): 3rd National Symposium of Gemology and Crystallography and Mineralogy, Shahid Beheshti University, Tehran, 31–36.
- Badr, A., Tabatabaei, M., Mackizadeh, M., Hashemi, M., M.A., and Taghipour, B., 2013, Mineralogical and geochemical studies of intrusive body of Ghohroud: *Petrology*, v. 4, p. 97–104. (*in Persian*).
- Bagdasaryan, G.P., and Gukasyan, P.X., 1962, The result of the absolute age determination of the separate magmatic complex of the Armyanskaya SSR, Nauka: Moscow and Leningrad, p. 283–303.
- Baharifar, A.A., 2011, Mineralogy and origin of garnet in acidic volcanic rocks of Dastgerd area, Qom: *Petrology*, v. 4, p. 1–14. (*in Persian*).
- Ballato, P., Uba, C.E., Landgraf, A., Strecker, M.R., Sudo, M., Stockli, D.F., Friedrich, A., and Tabatabaei, S.H., 2011, Arabia-Eurasia continental collision: Insights from late Tertiary foreland-basin evolution in the Alborz Mountains, northern Iran: *Bulletin*, v. 123, p. 106–131. doi:10.1130/B30091.1.
- Baxter, E.F., Caddick, M.J., and Ague, J.J., 2013, Garnet: Common mineral, uncommonly useful: *Elements*, v. 9, no. 6, p. 415–419. doi:10.2113/gselements.9.6.415.
- Berberian, F., and Berberian, M., 1981, Tectono-plutonic episodes in Iran: Zagros Hindu Kush Himalaya Geodynamic Evolution: Edited by Gupta, H.K., and Delany, F.M. American Geophysical Union, v.3, p.33–69.
- Berberian, M., and King, G.C.P., 1981, Towards a paleogeography and tectonic evolution of Iran: *Canadian Journal of Earth Sciences*, v. 18, no. 2, p. 210–265. doi:10.1139/e81-019.
- Bray, E.A., 1988, Garnet compositions and their use as indicators of peraluminous granitoid petrogenesis-southeastern Arabian Shield: Contributions to Mineralogy and Petrology, v. 100, p. 205–212. doi:10.1007/BF00373586.
- Brod, J.A., Junqueira-Brod, T.C., Gaspar, J.C., Gibson, S.A., and Thomson, R.N., 2003, Ti-rich and Ti-poor garnet from the Tapira Carbonatite Complex, SE Brazil: Fingerprinting fractional crystallisation and liquid immiscibility: In 8th International Kimberlite Conference, Victoria, British Columbia, Canada, Abstract.
- Burda, J., and Gawęda, A., 2009, Shear-influenced partial melting in the Western Tatra metamorphic complex: Geochemistry and geochronology: *Lithos*, v. 110, no. 1–4, p. 373–385. doi:10.1016/j.lithos.2009.01.010.
- Cartwright, I., and Oliver, N.H., 1994, Fluid flow during contact metamorphism at Mary Kathleen, Queensland, Australia: *Journal of Petrology*, v. 35, no. 6, p. 1493–1519. doi:10.1093/petrology/35.6.1493.
- Chappell, B.W., 1984, Source rocks of I- and S-type granites in the Lachlan Fold Belt, southeastern Australia: *Philosophical Transactions of the Royal Society of London: Series A, Mathematical and Physical Sciences*, v. 310, p. 693–707.
- Chavideh, M., Tabatabaei Manesh, S.M., and Mackizadeh, M.A., 2018, Petrology of skarns in the north and the southwest of Qazan (South Qamsar) with emphasis on the mineral chemistry of garnet and pyroxene: *Petrology*, v. 33, p. 111–132. (*in Persian*). doi:10.22108/ijp.2017.100423.0.
- Chen, X.H., and Zhao, Y.Q., 1991, Characteristics, genesis and petrogenic significance of garnet phenocrysts in acid lavas from the Xiling mining area: *Geochimica*, v. 1, p. 33–39.
- Chiu, H.Y., Chung, S.L., Zarrinkoub, M.H., Mohammadi, S.S., Khatib, M.M., and Iizuka, Y., 2013, Zircon U–Pb age constraints from Iran on the magmatic evolution related to Neotethyan subduction and Zagros orogeny: *Lithos*, v. 162, p. 70–87. doi:10.1016/j.lithos.2013.01.006.
- Cioni, R., Civetta, L., Marianelli, P., Metrich, N., Santacroce, R., and Sbrana, A., 1995, Compositional layering and syn-eruptive mixing of a periodically refilled shallow magma chamber: The AD 79 Plinian eruption of Vesuvius: *Journal of Petrology*, v. 36, no. 3, p. 739–776. doi:10.1093/petrology/36.3.739.

- Clemens, J.D., 1992, Partial melting and granulite genesis: A partisan overview: *Precambrian Research*, v. 55, no. 1–4, p. 297–301. doi:10.1016/0301-9268(92)90029-N.
- Clemens, J.D., 2003, S-type granitic magmas e petrogenetic issues, models and evidence: *Earth Science Review*, v. 61, p. 1–18. doi:10.1016/S0012-8252(02)00107-1.
- Clemens, J.D., and Wall, V.J., 1981, Origin and crystallization of some peraluminous (S-type) granitic magmas: *The Canadian Mineralogist*, v. 19, p. 111–131.
- Clemens, J.D., and Wall, V.J., 1984, Origin and evolution of a peraluminous silicic ignimbrite suite: The Violet Town Volcanics: *Contributions to Mineralogy and Petrology*, v. 88, no. 4, p. 354–371. doi:10.1007/BF00376761.
- Collins, W.J., and Hobbs, B.E., 2001, What caused the Early Silurian change from mafic to silicic (S-type) magmatism in the eastern Lachlan Fold Belt: *Australian Journal of Earth Sciences*, v. 48, no. 1, p. 25–41. doi:10.1046/j.1440-0952.2001.00837.x.
- Cox, K.G., Bell, J.D., and Pankhurst, R.J., 1979, The interpretation of igneous rocks: George Allen and Unwin
- D’Errico, M.E., Lackey, J.S., Surplless, B.E., Loewy, S.L., Wooden, J. L., Barnes, J.D., Strickland, A., and Valley, J.W., 2012, A detailed record of shallow hydrothermal fluid flow in the Sierra Nevada magmatic arc from low- $\delta^{18}O$ skarn garnets: *Geology*, v. 40, no. 8, p. 763–766. doi:10.1130/G33008.1.
- Dahlquist, J.A., Galindo, C., Pankhurst, R.J., Rapela, C.W., Alasino, P.H., Saavedra, J., and Fanning, C.M., 2007, Magmatic evolution of the Penon Rosado granite: Petrogenesis of garnet-bearing granitoids: *Lithos*, v. 95, no. 3–4, p. 177–207. doi:10.1016/j.lithos.2006.07.010.
- Dargahi, S., Arvin, M., Pan, Y., and Babaei, A., 2010, Petrogenesis of post-collisional A-type granitoids from the Urumieh–Dokhtar magmatic assemblage, Southwestern Kerman, Iran: Constraints on the Arabian–Eurasian continental collision: *Lithos*, v. 115, no. 1–4, p. 190–204. doi:10.1016/j.lithos.2009.12.002.
- Davoudian, A.R., Genser, J., Dachs, E., and Shabanian, N., 2008, Petrology of eclogites from north of Shahrekord, Sanandaj-Sirjan Zone, Iran: *Mineralogy and Petrology*, v. 92, no. 3–4, p. 393–413. doi:10.1007/s00710-007-0204-6.
- Dawson, J.B., Smith, J.V., and Steele, I.M., 1995, Petrology and mineral chemistry of plutonic igneous xenoliths from the carbonatite volcano, Oldoinyo Lengai, Tanzania: *Journal of Petrology*, v. 36, no. 3, p. 797–826. doi:10.1093/petrology/36.3.797.
- Day, R.A., Green, T.H., and Smith, I., 1992, The origin and significance of garnet phenocrysts and garnet-bearing xenoliths in Miocene calc alkaline volcanics from Northland, New-Zealand: *Journal of Petrology*, v. 33, p. 125–161. doi:10.1093/petrology/33.1.125.
- Deer, W.A., Howie, R.A., and Zussman, J., 1982, *Rock-Forming Minerals. Orthosilicates*, 2nd edn: Longman, New York, p. 1A
- Deer, W.A., Howie, R.A., and Zussman, J., 1992, *An Introduction to Rock Forming Minerals*: Harlow, England.
- Dingwell, D.B., and Brearley, M., 1985, Mineral chemistry of igneous melanite garnets from analcite-bearing volcanic rocks, Alberta, Canada: *Contributions to Mineralogy and Petrology*, v. 90, no. 1, p. 29–35. doi:10.1007/BF00373038.
- Douman, M., and Dirlam, D., 2004, Update on demantoid and cat’s-eye demantoid from Iran: *Gems and Gemology*, v. 40, p. 67–68.
- Du Toit, G., Mayerson, W., Van Der Bogert, C., Douman, M., Befi, R., Koivula, J.I., and Kiefert, L., 2006, Demantoid from Iran: *Gems and Gemology*, v. 42, p. 131.
- Einaudi, M.T., and Burt, D.M., 1982, Introduction; terminology, classification, and composition of skarn deposits: *Economic Geology*, v. 77, no. 4, p. 745–754. doi:10.2113/gsecongeo.77.4.745.
- Esmaily, D., Nedelec, A., Valizadeh, M.V., Moore, F., and Cotten, J., 2005, Petrology of the Jurassic Shah-Kuh granite (eastern Iran), with reference to tin mineralization: *Journal of Asian Earth Sciences*, v. 25, no. 6, p. 961–980. doi:10.1016/j.jseaes.2004.09.003.
- Fallah Karimi, Z., 2012, Mineralogy and geochemistry of Ghinargeh iron index (NE of Takab, West-Azarbaidjan province) [MSc. thesis], University of Urmia Faculty of Sciences. (*in Persian*).
- Fatehi, H., and Ahmadipour, H., 2017, Reconstruction of geological setting for the photolith of Gol-Gohar, Ruchun and Khabar metamorphic complex (South-west of Baft, Kerman province): *Scientific Quarterly Journal, Geosciences*, v. 27, p. 253–264. (*in Persian*)
- Ferdowsi, R., Calagari, A.A., Hosseinzadeh, G., and Sohrabi, G., 2012, Studies of petrography, metasomatic alteration, and genesis of Kamtal iron-copper skarn, northeast of Kharvana, east-Azarbaijan: *Economic Geology*, v. 4, p. 47–58. (*in Persian*). doi:10.22067/econg.v4i1.13392.
- Ferdowsi, R., Moayyed, M., and Kamali, A., 2015, Investigation of petrography, petrogenesis and geochemical features of Kalaibar nepheline syenitic body, Kalaibar, east Azarbaijan: *Scientific Quarterly Journal, Geosciences*, v. 24, p. 29–40. (*in Persian*).
- Fulignati, P., Marianelli, P., Santacroce, R., and Sbrana, A., 2004, Probing the Vesuvius magma chamber–host rock interface through xenoliths: *Geological Magazine*, v. 141, p. 417–428.
- Ghanei Ardakaneji, J., and Mackizadeh, M.A., 2011, Textural assemblage relationships between Clintonite-spinel-garnet in the Central Iranian skarns as evidence of clintonite genesis: *Petrology*, v. 4, p. 65–72. (*in Persian*).
- Ghanei Ardakani, J., Mahdizadeh Shahri, H., Darvishzadeh, A., and Mackizadeh, M.A., 2014, Petrography and petrogenesis of Hasht-Kuh Khezrabad of Yazd Skarns: *Petrology*, v. 17, p. 69–82. (*in Persian*)
- Gharsi, M., Rasa, I., and Yazdi, M., 2018, Investigation of Mazraeh Skarn mineralization, North of Ahar, with an emphasis on fluid inclusion studies: *Iranian Journal of Crystallography and Mineralogy*, v. 26, p. 229–244. (*in Persian*).
- Ghazi, A.M., and Hassanipak, A.A., 1999, Geochemistry of sub-alkaline and alkaline extrusives from the Kermanshah ophiolite, Zagros Suture Zone, Western Iran: Implications for Tethyan plate tectonics: *Journal of Asian Earth Sciences*, v. 17, no. 3, p. 319–332. doi:10.1016/S0743-9547(98)00070-1.
- Ghorbani, M., 2003, *Precious stones and minerals (gemstones) and their position in Iran*: Pars Geology Research Center, Tehran, Iran, p. 396.
- Gilg, H.A., Boni, M., Balassone, G., Allen, C.R., Banks, D., and Moore, F., 2006, Marble-hosted sulfide ores in the Angouran Zn-(Pb-Ag) deposit, NW Iran: Interaction of sedimentary brines with a metamorphic core complex: *Mineral Deposita*, v. 41, no. 1, p. 1–16. doi:10.1007/s00126-005-0035-5.
- Gukusyan, R.X., 1963, Determination of the absolute age by Rb-Sr method on a sample from the Megrinsky pluton Armenian SSR: *Seriya Geologiya Erevan*, v. 36, p. 173–178.

- Gwalani, L.G., Rock, N.M.S., Ramaswamy, R., Griffin, B.J., and Mulai, B.P., 2000, Complexly zoned Ti-rich melanite-schorlomite garnets from Ambadungar carbonatite-alkalic complex, Deccan Igneous Province, Gujarat State, western India: *Journal of Asian Earth Sciences*, v. 18, p. 163–176. doi:10.1016/S1367-9120(99)00053-X.
- Hajialioghli, R., Moazzen, M., Droop, G.T.R., Oberhancli, R., Bousquet, T.R., Jahangiri, A., and Ziemman, M., 2007a, Serpentine polymorphs and P-T evolution of metaperidotites and serpentinites in the Takab area, NW Iran: *Mineralogical Magazine*, v. 71, p. 203–222.
- Hajialioghli, R., 2018, Mineral chemistry, P-T and tectonometamorphic evolutions of garnet amphibolites from the Takht-e-Soleyman, NW Takab: *Iranian Journal of Crystallography and Mineralogy*, v. 25, p. 749–760. (*in Persian*).
- Hajialioghli, R., and Moazzen, M., 2009, Heterogeneous garnets in the alkaline feldspathoid-bearing rocks from the Kaleybar pluton, northern Azerbaijan (NW Iran): *Iranian Journal of Crystallography and Mineralogy*, v. 17, p. 203–212. (*in Persian*).
- Hajialioghli, R., Moazzen, M., Jahangiri, A., Droop, G.T.R., Bousquet, R., and Oberhansli, R., 2007b, August. Petrogenesis of meta-peridotites in the Takab area, NW Iran: In *Goldschmidt Conference Abstracts, Germany* p.A (370).
- Hajialioghli, R., Moazzen, M., Jahangiri, A., Oberhansli, R., Mocek, B., and Altenberger, U., 2011, Petrogenesis and tectonic evolution of metaluminous sub-alkaline granitoids from the Takab Complex, NW Iran: *Geological Magazine*, v. 148, no. 2, p. 250–268. doi:10.1017/S0016756810000683.
- Harangi, S., Downes, H., Kosa, L., Szabo, C., Thirlwall, M.F., Mason, P.R.D., and Matthey, D., 2001, Almandine garnet in calc-alkaline volcanic rocks of the Northern Pannonian Basin (Eastern-Central Europe): *Geochemistry, petrogenesis and geodynamic implications: Journal of Petrology*, v. 42, p. 1813–1843. doi:10.1093/petrology/42.10.1813.
- Harley, S.L., 1998, On the occurrence and characterisation of ultrahigh temperature (UHT) crustal metamorphism, in Treloar, P.J., and O'Brien, P., eds., *What Controls Metamorphism and Metamorphic Reactions*, volume Vol. 138: Special Publication Geological Society of London, p. 75–101.
- Harrison, T.N., 1988, Magmatic Garnets in the Cairngorn Granite, Scotland: *Mineralogical Magazine*, v. 52, no. 368, p. 659–667. doi:10.1180/minmag.1988.052.368.10.
- Honarmand, M., Rashidnejad Omran, N., Corfu, F., et al., 2013, Geochronology and Magmatic History of a Calc-Alkaline Plutonic Complex in the Urumieh-Dokhtar Magmatic Belt, Central Iran: Zircon Ages as Evidence for Two Major Plutonic Episodes: *Neues Jahrbuch Für Mineralogie Abhandlungen*, v. 190, p. 67–77. doi:10.1127/0077-7757/2013/0230.
- Hosseini, M.R., Alirezaei, S., and Hassanzadeh, J., 2017, Mineralization and geochemical characteristics of ore-forming fluids in Bahr Aseman area, southeast of Kerman magmatic belt: *Scientific Quarterly Journal, Geosciences*, v. 27, p. 143–156. (*in Persian*)
- Howie, R.A., and Woolley, A., 1968, The role of titanium and the effect of TiO₂ on the cell-size, refractive index and specific gravity in the andradite-melanite-schorlomite series: *Mineralogical Magazine*, v. 36, p. 775–970. doi:10.1180/minmag.1968.036.282.04.
- Huggins, F.E., Virgo, D., and Huckenholz, H.G., 1977a, Titanium containing silicate garnets. I. The distribution of Al, Fe³⁺, and Ti⁴⁺ between octahedral and tetrahedral sites: *American Mineralogist*, v. 62, p. 475–490.
- Huggins, F.E., Virgo, D., and Huckenholz, H.G., 1977b, Titanium containing silicate garnets. II. The crystal chemistry of melanites and schorlomes: *American Mineralogist*, v. 62, p. 646–655.
- Jamshidzaei, A., Mackizadeh, M.A., and Ayati, F., 2017, Paragenesis relations study of wollastonite – Pyroxene – Garnet mineral assemblage in Vegeh Skarn (North East Isfahan): *Petrology*, v. 30, p. 1–14. (*in Persian*). doi:10.22108/ijp.2017.81938.
- Jamtveit, B., and Hervig, R.L., 1994, Constraints on transport and kinetics in hydrothermal systems from zoned garnet crystals: *Science*, v. 263, p. 505–508. doi:10.1126/science.263.5146.505.
- Jung, D., Keller, J., Khorassani, R., Chr., M., Bumann, A., and Horn, P.L., 1985, Petrology of Tertiary magmatic activity in northern Lut area, East of Iran: *Geological Survey of Iran Report*, v. 51, p. 285–336.
- Jung, S., and Hellebrand, E., 2006, Trace element fractionation during high-grade metamorphism and crustal melting-constraints from ion microprobe data of metapelitic, migmatitic and igneous garnets and implications for SmNd garnet chronology: *Lithos*, v. 87, p. 193–213. doi:10.1016/j.lithos.2005.06.013.
- Jung, S., Mezger, K., and Hoernes, S., 2001, Trace element and isotopic (Sr, Nd, Pb, O) arguments for a mid-crustal origin of Pan-African garnetbearing S-type granites from the Damara orogen (Namibia): *Precambrian Research*, v. 110, p. 325–355. doi:10.1016/S0301-9268(01)00175-9.
- Kawabata, H., and Takafuji, N., 2005, Origin of garnet crystals in calc-alkaline volcanic rocks from the Setouchi volcanic belt, Japan: *Mineralogical Magazine*, v. 69, no. 6, p. 951–971. doi:10.1180/0026461056960301.
- Kebede, T., Koeberl, C., and Koller, F., 2001, Magmatic evolution of the SuquiiWagaa garnet-bearing two-mica granite, wallagga area, western Ethiopia: *Journal of African Earth Sciences*, v. 32, no. 2, p. 193–221. doi:10.1016/S0899-5362(01)90004-1.
- Lackey, J.S., Valley, J.W., and Hinke, H.J., 2006, Deciphering the source and contamination history of peraluminous magmas using italic type ¹⁸O of accessory minerals: Examples from garnet-bearing plutons of the Sierra Nevada batholith: *Contributions to Mineralogy and Petrology*, v. 151, p. 20–44. doi:10.1007/s00410-005-0043-6.
- Lang, J.R., Lueck, B., Mortensen, J.K., Kelly Russell, J., Stanley, C. R., and Thompson, J.F., 1995, Triassic-Jurassic silica-undersaturated and silica-saturated alkalic intrusions in the Cordillera of British Columbia: Implications for arc magmatism: *Geology*, v. 23, p. 451–454.
- Lotfi, M., 2001, Geological map of Iran, 1:100,000 series sheet, Takht-e-Soleiman: Tehran, Geological Survey of Iran.
- Mahmoudi, S., and Azadbakht, S., 2015, Atoll garnets petrogenesis in the Boland parchen metamorphic complex in southwest Mahneshan: *Iranian Journal of Crystallography and Mineralogy*, v. 23, p. 189–198. (*in Persian*).
- Mahmoudi, S., Corfu, F., Masoudi, F., Mehrabi, B., and Mohajjel, M., 2011, U–Pb dating and emplacement history

- of granitoid plutons in the northern Sanandaj–Sirjan Zone, Iran: *Journal of Asian Earth Sciences*, v. 41, no. 3, p. 238–249. doi:10.1016/j.jseaes.2011.03.006.
- Makizadeh, M.A., Rahgoshay, M., and Daliran, F., 2007, Genesis of andradite garnets from Surk Fe skarn, Nain-Surk ophiolite belt: *Res: Journal of Universal. Isfahan Sciences*, v. 27, p. 157–167.
- Malehmir, P., 2016, Investigation the possibility of natural andradite crystal growth as synthetic demantoid [M.Sc thesis]: Kharazmi University. (*in Persian*).
- Maleki, S., Alirezaei, S., and Corfu, F., 2019, Dating of Oligocene granitoids in the Khak-Sorkh area, Central Urumieh-Dokhtar arc, Iran, and a genetic linkage with the associated skarn iron deposit: *Journal of Asian Earth Sciences*, v. 182, p. 103930. doi:10.1016/j.jseaes.2019.103930.
- Maniar, P.D., and Piccoli, P.M., 1989, Tectonic discrimination of granitoids: *Geological Society of America Bulletin*, v. 101, p. 635–643. DOI: 10.1130/B-101-1989-02.
- Manning, P.G., and Harris, D.C., 1970, Optical absorption and electron-microprobe studies of some high Ti Andradites: *Canadian Mineralogist*, v. 10, p. 260–271.
- Mazhari, S.A., Bea, F., Amini, S., Ghalamghash, J., Molina, J.F., Montero, P., Scarrow, J.H., and Williams, I.S., 2009, The Eocene bimodal Piranshahr massif of the Sanandaj–Sirjan Zone, NW Iran: A marker of the end of the collision in the Zagros orogeny: *Journal of the Geological Society*, v. 166, no. 1, p. 53–69. doi:10.1144/0016-76492008-022.
- Meagher, E.P., 1982, Silicate garnets, in Ribbe, P.H., ed., *Orthosilicates: Review in Mineralogy*, volume Vol. 5: p. 25–66
- Meen, V.B., and Tushingham, A.D., 1968, *Crown Jewels of Iran*: University of Toronto Press, Toronto
- Mehdizadeh Shahri, H., Ghanei Ardakane, J., Darvishzadah, A., and Mackizadeh, M.A., 2014, Petrography and petrogenesis of Hasht-kuh Khezrabad of Yazd skarns: *Petrology*, v. 17, p. 69–82. (*in Persian*).
- Méndez-Ortiz, B.A., Carrillo-Chávez, A., Monroy-Fernández, M. G., and Levresse, G., 2012, Influencia del pH y la alcalinidad en la adsorción de As y metales pesados por oxihidróxidos de Fe en jales mineros de tipo skarn de Pb-Zn-Ag: *Revista Mexicana De Ciencias Geológicas*, v. 29, p. 639–648.
- Miller, C.F., and Stoddard, E.F., 1981, The role of manganese in the paragenesis of magmatic garnet: An example from the Old Woman-Piute Range, California: *The Journal of Geology*, v. 89, no. 2, p. 233–246. doi:10.1086/628582.
- Mirnejad, H., Blourian, G.H., Kheirkhah, M., Akrami, M.A., and Tutti, F., 2008, Garnet-bearing rhyolite from Deh-Salm area, Lut block, Eastern Iran: Anatexis of deep crustal rocks: *Mineralogy and Petrology*, v. 94, no. 3–4, p. 259–269. doi:10.1007/s00710-008-0015-4.
- Moazzen, M., and Hajialioghli, R., 2008, Zircon SHRIMP dating of mafic migmatites from NW Iran: Reporting the oldest rocks from the Iranian crust: 5th Annual Meeting AOGS, Busan, Korea SE62.
- Moazzen, M., Oberhänsli, R., Hajialioghli, R., Möller, A., Bousquet, R., Droop, G., and Jahangiri, A., 2009, Peak and post-peak P–T conditions and fluid composition for scapolite-clinopyroxene-garnet calc-silicate rocks from the Takab area, NW Iran: *European Journal of Mineralogy*, v. 21, p. 149–162. doi:10.1127/0935-1221/2009/0021-1887.
- Moeinzadeh, S.H., Rahimisadeh, H., and Moazzen, M., 2019, The Study of amphibolites in Bahram Gor area (northwest of Gol-e Gohar mine in Sirjan), with emphasis on mineral paragenesis and whole rock chemical data: *Petrology*, v. 36, p. 49–66. (*in Persian*)
- Moghadam, H., Bröcker, M., Griffin, W.L., Li, X.H., Chen, R.X., and O'Reilly, S.Y., 2017, Subduction, high-P metamorphism, and collision fingerprints in South Iran: Constraints from zircon U–Pb and mica Rb–Sr geochronology: *Geochemistry Geophysics Geosystem*, v. 18, p. 306–332. doi:10.1002/2016GC006585.
- Moghadam, H., Mosaddegh, H., and Santosh, M., 2013, Geochemistry and petrogenesis of the Late Cretaceous Haji-Abad ophiolite (Outer Zagros Ophiolite Belt, Iran): Implications for geodynamics of the Bitlis–Zagros suture zone: *Geological Journal*, v. 48, p. 579–602.
- Mohammaddoost, H., Ghaderi, M., and Rashidnejad Omran, N., 2015, Determining the origin of mineralizing fluid at Qamsar cobalt deposit using fluid inclusions and S–O stable isotopes: *Scientific Quarterly Journal, Geosciences*, v. 24, p. 235–248. (*in Persian*). doi:10.22071/gsj.2015.41769.
- Mokhtari, M.A.A., 2012, The Mineralogy and Petrology of the Pahnavar Fe skarn, In the Eastern Azarbaijan, NW Iran: *Central European Journal of Geosciences*, v. 4, p. 578–591. doi:10.2478/s13533-012-0106-y.
- Montaseri, M., 2011, Mineralogy, geochemistry, genesis and geological origin of green garnets of Esfandagheh ophiolites (southeast Kerman) [M.Sc thesis]: Shiraz University. (*in Persian*).
- Montaseri, M., Etemadi, B., and Mousavinasab, Z., 2013, Introducing andradites of Iran (Soghan) with the quality of jewelry and comparing it with other examples of the world. 17th Symposium of Geological Society of Iran: Shahid Beheshti University, Tehran.
- Montel, J.M., and Vielzeuf, D., 1997, Partial melting of meta-greywackes. 2. compositions of minerals and melts: *Contributions to Mineralogy and Petrology*, v. 128, p. 176–196. doi:10.1007/s004100050302.
- Moore, F., Deymar, S., and Taghipour, B., 2012a, Genetic relation between skarn mineralization and petrogenesis of the Darreh Zerreshk granitoid intrusion, southwest of Yazd: *Economic Geology*, v. 3, p. 97–110. (*in Persian*).
- Moore, F., Deymar, S., and Taghipour, B., 2012b, Geochemistry of Rare Earth Elements and mineral chemistry of garnet in Darreh Zerreshk skarns: *Iranian Journal of Crystallography and Mineralogy*, v. 3, p. 431–444. (*in Persian*).
- Moradian, A., Peighambari, S., and Ahmadipour, H., 2005, Petrology, mineral chemistry and petrogenesis of metapelites of Tanbour metamorphic complex, east of Sirjan (Kerman province): *Iranian Journal of Crystallography and Mineralogy*, v. 2, p. 347–362. (*in Persian*).
- Moritz, R., Ghazban, F., and Singer, B.S., 2006, Eocene gold ore formation at Muteh, Sanandaj–Sirjan tectonic zone, Western Iran: A result of late-stage extension and exhumation of metamorphic basement rocks within the Zagros Orogen: *Economic Geology*, v. 101, p. 1497–1524.
- Moshtagh, S., Jamali, H., Nadimi Shahraki, A., Bagheri, H., and Baniadam, F., 2017, Genesis and tectono-magmatic setting of Sadrabad iron Skarn (west of Yazd): *Petrology*, v. 28, p. 55–72. (*in Persian*)
- Nadimi, A., 2007, Evolution of the Central Iranian basement: *Gondwana Research*, v. 12, no. 3, p. 324–333. doi:10.1016/j.gr.2006.10.012.
- Naimo, D., Balassone, G., Beran, A., Amalfitano, C., Imperato, M., and Stanzione, D., 2003, Garnets in volcanic breccias of the Phlegraean Fields (southern Italy): *Mineralogical,*

- geochemical and genetic features: *Mineralogy and Petrology*, v. 77, no. 3–4, p. 259–270. doi:10.1007/s00710-002-0219-y.
- Nash, C.R., 1972, Primary anhydrite in Precambrian gneisses from the Swakopmund district, South West Africa: *Contributions to Mineralogy and Petrology*, v. 36, no. 1, p. 27–32. doi:10.1007/BF00372832.
- Patino- Douce, A.E., and Beard, J.S., 1996, Effects of P, (fO₂) and Mg/Fe ratios on dehydration melting of model metagreywackes: *Journal of Petrology*, v. 37, p. 999–1024. doi:10.1093/petrology/37.5.999.
- Pearce, J.A., Harris, N.B., and Tindle, A.G., 1984, Trace element discrimination diagrams for the tectonic interpretation of granitic rocks: *Journal of Petrology*, v. 25, no. 4, p. 956–983. doi:10.1093/petrology/25.4.956.
- Pearl, R.M., 1975, *Garnet: Gemstones and Minerals: USA*.
- Peighambari, S., Jamshidi Badr, M., and Heidarian, H., 2012, The Petrofabric and geochemistry of garnet porphyroblast in Khajoo and Tanbor metamorphic complexes (East Sirjan): 6th National Geological Conference of Payam Noor University, Kerman, PNUGEO6-B-28.
- Perfiliev, Y., Aistov, L., and Selivanov, E., 1979, *Geology and minerals of Khur area (central Iran)*, volume Vol. 3, p. 325. Moscow, V/O Technoexport, Report.
- Pirajno, F., 2013, Effects of metasomatism on mineral systems and their host rocks: Alkali metasomatism, skarns, greisens, tourmalinites, rodingites, black-wall alteration and listvenites, in *Metasomatism and the Chemical Transformation of Rock*: Berlin, Heidelberg, Springer, p. 203–251.
- Plank, T., 1987, Magmatic garnets from the Cardigan pluton and the Acadian thermal event in southwest New-Hampshire: *American Mineralogist*, v. 72, p. 681–688.
- Rahgoshay, M., Mackizadeh, M.A., Amoi Ardekani, T., and Moghadam, H., 2008, Geochemical study of garnet-vesuvianite-wollastonite-pyroxene mineral assemblage in Hosh Skarns, west of Taft (Yazd): *Iranian Journal of Crystallography and Mineralogy*, v. 16, p. 31–48. (in Persian).
- Rahimisadegh, H., Moeinzadeh, H., and Moazzen, M., 2018, Studying of geology, petrography, whole rock chemistry and petrogenesis of metasediments in the region of Bahram Gor, Sirjan: 2th National conference on Geology and Mineral Exploration. Kerman Institute of Higher Education, Kerman, Iran.
- Rahimisadegh, H., Moeinzadeh, S.H., and Moazzen, M., 2014, Petrographic Studying of garnet porphyroblasts of schists in Bahram Gur Sirjan area to determine the metamorphic phases: 1th National Conference on Gemology-Crystallography of Iran, Shahid Bahonar University of Kerman, Iran.
- Rahimzadeh, B., 2016, Introduce and pay attention to collection minerals in Iran. 3rd National symposium of gemology and crystallography of Iranian Society of Crystallography and Mineralogy, Shahid Beheshti University, Tehran, Iran.
- Ranjbar, S., Tabatabaei Manesh, S.M., and Mackizadeh, M.A., 2015, Mineralogy of garnet in Khuni skarn, northeast of Anarak, Isfahan province: Evidences for a Hydrothermal System Evolution: *Scientific Quarterly Journal, Geosciences*, v. 25, p. 173–182. (in Persian). doi:10.22071/gsj.2015.41423.
- Ranjbar, S., Tabatabaei Manesh, S.M., Mackizadeh, M.A., Tabatabaei, S.H., and Parfenova, O.V., 2016, Geochemistry of major and rare earth elements in garnet of the Kal-e Kafi Skarn, Anarak Area, Central Iran: Constraints on processes in a hydrothermal system: *Geochemistry International*, v. 54, no. 5, p. 423–438. doi:10.1134/S0016702916050098.
- Russell, J.K., Dipple, G.M., Lang, J.R., and Lueck, B., 1999, Major-element discrimination of titanium andradite from magmatic and hydrothermal environments; An example from the Canadian Cordillera: *European Journal of Mineralogy*, v. 11, no. 6, p. 919–935. doi:10.1127/ejm/11/6/0919.
- Saccani, N., Visintin, F., and Rapaccini, M., 2014, Investigating the linkages between service types and supplier relationships in servitized environments: *International Journal of Production Economics*, v. 149, p. 226–238. doi:10.1016/j.ijpe.2013.10.001.
- Safarzadeh, E., Masoudi, F., Hassanzadeh, J., and Pourmoafi, S. M., 2016, The presence of Precambrian basement in Gol Gohar of Sirjan (south of Iran): *Petrology*, v. 26, p. 153–170. (in Persian)
- Saha, A., Ray, J., Ganguly, S., and Chatterjee, N., 2011, Occurrence of melanite garnet in syenite and ijolite–melteigite rocks of Samchampi–Samteran alkaline complex, Mikir Hills, Northeastern India: *Current Science*, p. 95–100.
- Saki, A., 2010, Proto-Tethyan remnants in northwest Iran: Geochemistry of the gneisses and metapelitic rocks: *Gondwana Research*, v. 17, no. 4, p. 704–714. doi:10.1016/j.gr.2009.08.008.
- Saki, A., and Moazzen, M., 2009, Study of mineral chemistry and thermobarometry of Boland Parchin granitoids, NW Iran: *Iranian Journal of Crystallography and Mineralogy*, v. 16, p. 652–663. (in Persian).
- Saki, A., Moazzen, M., Modjtahedi, M., and Oberhänsli, R., 2008, Determination of P–T conditions of metamorphism of Mahneshan Complex, NW Iran: *Iranian Journal of Geosciences*, v. 68, p. 80–94. doi:10.1002/gj.1236.
- Sarjoughian, F., and Kananian, A., 2017, Zircon U–Pb geochronology and emplacement history of intrusive rocks in the Ardestan section, central Iran: *Geologica Acta: An International Earth Science Journal*, v. 15, p. 25–36. doi:10.1344/GeologicaActa2017.15.1.3.
- Sarjoughian, F., Lentz, D., Kananian, A., Ao, S., and Xiao, W., 2018, Geochemical and isotopic constraints on the role of juvenile crust and magma mixing in the UDMA magmatism, Iran: Evidence from mafic microgranular enclaves and cogenetic granitoids in the Zafarghand igneous complex: *International Journal of Earth Sciences*, v. 107, no. 3, p. 1127–1151. doi:10.1007/s00531-017-1548-8.
- Scheibner, B., Wörner, G., Civetta, L., Stosch, H.G., Simon, K., and Kronz, A., 2007, Rare earth element fractionation in magmatic Ca-rich garnets: Contributions to Mineralogy and Petrology, v. 154, p. 55–74. doi:10.1007/s00410-006-0179-z.
- Sengör, A.M.C., 1987, Tectonics of the Tethysides: Orogenic collage development in a collisional setting: *Annual Review of Earth and Planetary Sciences*, v. 15, p. 213–244. doi:10.1146/annurev.earth.15.1.213.
- Sepidbar, F., Ao, S., Palin, R.M., Li, Q.L., and Zhang, A., 2018, Origin age and petrogenesis of barren low-grade) granitoids from the Bezenjan-Bardsir magmatic complex, southeast of the Urumieh-Dokhtar magmatic belt, Iran: *Ore Geology Review*, v. 104, p. 132–147. doi:10.1016/j.oregeorev.2018.10.008.
- Shafiei, B., Haschke, M., and Shahabpour, J., 2009, Recycling of orogenic arc crust triggers porphyry Cu mineralization in Kerman Cenozoic arc rocks, southeastern Iran: *Mineralium Deposita*, v. 44, no. 3, p. 265–283. doi:10.1007/s00126-008-0216-0.

- Shahsavari, A.B., Rashidnejad-Omran, N., Toksoy-Köksal, F., Xu, W., and Ghalamghash, J., 2019, Oligocene subduction-related plutonism in the Nodoushan area, Urumieh-Dokhtar magmatic belt: Petrogenetic constraints from U–Pb zircon geochronology and isotope geochemistry: *Geoscience Frontiers*, v. 10, no. 2, p. 725–751. doi:10.1016/j.gsf.2018.03.017.
- Shang, L., 2010, Demantoid garnet Cats eye from Iran and Russia: *The Journal of Gemological Association of Hong Kong*, p. 74–78.
- Sheibi, M., Esmaily, D., and Nedele, A., 2009, Magmatic evolution of granites from Shir-Kuh area, Yazd block, Central Iran: Anatexis of deep crustal rocks: *Geochimica Et Cosmochimica Acta Supplement*, v. 73, p. A1207.
- Sheibi, M., Esmaily, D., Nédélec, A., Bouchez, J.L., and Kananian, A., 2010, Geochemistry and petrology of garnet-bearing S-type Shir-Kuh Granite, southwest Yazd, Central Iran: *Island Arc*, v. 19, p. 292–312. doi:10.1111/j.1440-1738.2010.00707.
- Sherafat, S., and Mackizadeh, M.A., 2017, Mineralogy and Genesis of Joveinan Iron Skarn (Cenozoic Magmatic Arc, North of Isfahan: *Petrology*, v. 29, p. 89–108. (in Persian).
- Sinkankas, J., 1961, *Gemstones and Minerals*: New York
- Sinkankas, J., 1972, *Gemstone and Mineral Data Book*: New York
- Smith, G.F.H., and Phillips, F.C., 1972, *Gemstones*, 14th Edition: London.
- Smith, M.P., Henderson, P., Jeffries, T.E.R., Long, J., and Williams, C.T., 2004, The rare earth elements and uranium in garnets from the Beinn and Dubhaich Aureole, Skye, Scotland, UK: Constraints on processes in a dynamic hydrothermal system: *Journal of Petrology*, v. 45, p. 457–484. doi:10.1093/petrology/egg087.
- Sohrabi, G., Hosseinzadeh, M.R., Calagari, A.A., and Hajalilou, B., 2015, Study of Mo mineralization in Gharedagh (Ordobad)-Shivardagh strip with emphasis on alteration, petrology, and geochemistry of host intrusive bodies (Northwest of Iran): *Scientific Quarterly Journal, Geosciences*, v. 24, p. 243–258. (in Persian).
- Speer, J.A., and Becker, S.W., 1992, Evolution of magmatic and subsolidus AFM mineral assemblages in granitoid rocks: Biotite, muscovite, and garnet in the Cuffytown Creek pluton, South Carolina: *American Mineralogist*, v. 77, p. 821–833.
- Stampfli, G.M., 2000, *Tethyan oceans*: Geological society, volume Vol. 173: London, Special Publications, p. 1–23. doi:10.1144/GSL.SP.2000.173.01.01.
- Stockli, D.F., Hassanzadeh, J., Stockli, L.D., Axen, G., Walker, J.D., and Dewane, T.J., 2004, Structural and geochronological evidence for Oligo-Miocene intra-arc low-angle detachment faulting in the Takab–Zanjan area, NW Iran. Abstracts with programs: *Geological Society of America*, v. 36, p. 319.
- Stöcklin, J., 1968, Structural history and tectonics of Iran: A review: *American Association of Petroleum Geologists*, v. 52, p. 1229–1258.
- Stöcklin, J., and Nabavi, M.H., 1973, Tectonic map of Iran: *Geology Survey of Iran*.
- Stockton, C.M., and Mason, D.V., 1982, Gem garnets: The orange to red-orange color range. In: *Proceedings of the 1982 International Gemological Symposium*, GIA, Santa Monica, CA p.327–338.
- Štubňa, J., Bačík, P., Fridrichová, J., Hanus, R., Illášová, L., Milovská, S., Škoda, R., Vaculovič, T., and Ad Čerňanský, S., 2019, Gem-Quality Green Cr-Bearing Andradite (var. Demantoid) from Dobšiná, Slovakia: *Minerals*, v. 9, no. 3, p. 164. doi:10.3390/min9030164.
- Sylvester, P.J., 1998, Post-collisional strongly peraluminous granites: *Lithos*, v. 45, no. 1–4, p. 29–44. doi:10.1016/S0024-4937(98)00024-3.
- Tabatabaei Manesh, S.M., Mackizadeh, M.A., Ranjbar, S., and Gholinezhad, R., 2018, Mineralogy and determination of thermodynamic conditions at Javinan skarn, south of Kashan: *Scientific Quarterly Journal, Geosciences*, v. 28, p. 327–339. (in Persian). doi:10.22071/gsj.2017.72014.1008.
- Taghipour, B., Moore, F., Mackizadeh, M.A., and Taghipour, S., 2013, Hydrothermal garnet in porphyry copper related skarn deposits, Ali-Abad, Yazd Province, Iran: *Iranian Journal of Science and Technology*, v. A1, p. 11–22.
- Talebi, L., Mokhtari, M.A.A., Ebrahimi, M., and Kouhestani, H., 2017, The Arpachay mineralization occurrence, north of Takab: An epithermal base metal mineralization in the Takab-Angouran-Takht-e-Soleyman metallogenic zone: *Scientific Quarterly Journal, Geosciences*, v. 26, p. 281–296. (in Persian).
- Turbeville, B.N., 1993, Petrology and Petrogenesis of the Latera Caldera, Central Italy: *Journal of Petrology*, v. 34, no. 1, p. 77–124. doi:10.1093/petrology/34.1.77.
- Verdel, C., Wernicke, B.P., Hassanzadeh, J., and Guest, B., 2011, A Paleogene extensional arc flare-up in Iran: *Tectonics*, v. 30, p. 3. doi:10.1029/2010TC002809.
- Vincent, S.J., Allen, M.B., Ismail-Zadeh, A.D., Flecker, R., Foland, K.A., and Simmons, M.D., 2005, Insights from the Talysh of Azerbaijan into the Paleogene evolution of the South Caspian region: *Geological Society of America Bulletin*, v. 117, no. 11, p. 1513–1533. doi:10.1130/B25690.1.
- Wang, R.C., Hu, H., Zhang, A.C., Xu, S.J., and Wang, D.Z., 2003, Yttrium zoning in garnet from the Xihuashan granitic complex and its petrological implications: *Chinese Science Bulletin*, v. 48, no. 15, p. 1611–1615. doi:10.1007/BF03183970.
- Webster, R., 1983, *Gems, their Sources, Descriptions and Identification*, 4th Edition: London.
- Whitney, D.L., and Evans, B.W., 2010, Abbreviations for names of rock forming minerals: *American Mineralogist*, v. 95, p. 77–185. doi:10.2138/am.2010.3371.
- Whitworth, M.P., 1992, Petrogenetic implications of garnets associated with lithium pegmatites from SE Ireland: *Mineralogical Magazine*, v.56,p.75–83. doi:10.1180/minmag.1992.056.382.10.
- Woolley, A.R., 1973, The pseudo-leucite Borolanites and associated rocks of the south-eastern tract of the Borralan complex, Scotland: *Bulletin of the British Museum (Natural History)*, v. 2, p. 285–333.
- Wu, F.Y., Sun, D.Y., Jahn, B.M., and Wilde, S., 2004, A Jurassic garnet-bearing granitic pluton from NE China showing tetrad REE patterns: *Journal of Asian Earth Sciences*, v. 23, p. 731–744. doi:10.1016/S1367-9120(03)00149-4.
- Yu, J.H., Zhao, L., and Zhou, X., 2004, Mineralogical characteristics and origin of garnet-bearing I-type granitoids in south-eastern Fujian province: *Geological Journal of China Universities*, v. 10, p. 364–377.
- Yuan, C., Sun, M., Xiao, W.J., Wilde, S., Li, X.H., Liu, X.H., Long, X. P., Xia, X.P., Ye, K., and Li, J.L., 2009, Garnet-bearing tonalitic porphyry from East Kunlun, northeast Tibetan Plateau:

- Implications for adakite and magmas from the mash zone: *International Journal of Earth Sciences*, v. 98, no. 6, p. 1489–1510. doi:[10.1007/s00531-008-0335-y](https://doi.org/10.1007/s00531-008-0335-y).
- Zahedi, A., and Boomeri, M., 2013, Petrography, Petrogenesis and Geochemistry of Panah Kuh Skarn, West of Yazd: *Iranian Journal of Crystallography and Mineralogy*, v. 2, p. 267–276. (in Persian)
- Zahedi, A., and Boomeri, M., 2014, Studies on fluid inclusions and stable isotopes (C, O and S) during generation and evolution of Khut copper skarn West of Yazd, Central Iran: *Petrology*, v. 5, p. 107–126. (in Persian).
- Zahedi, A., and Boomeri, M., 2016, Water/rock interaction in Panah-Kuh skarn using Carbon and oxygen stable isotopes in different calcite types, west of Yazd: *Iranian Journal of Geology*, v. 37, p. 15–29. (in Persian).
- Zahedi, A., Boomeri, M., and Mackizadeh, M.A., 2013, REE geochemistry in skarn garnets from Khut and Panah-Kuh Ore deposit, West of Yazd: *Petrology*, v. 4, p. 47–66. (in Persian)
- Zahedi, A., Boomeri, M., Nakashima, K., Mackizadeh, M.A., Ban, M., and Lentz, D.R., 2014, Geochemical Characteristics, Origin, and Evolution of Ore-Forming Fluids of the Khut Copper Skarn Deposit, West of Yazd in Central Iran: *Resource Geology*, v. 64, no. 3, p. 209–232. doi:[10.1111/rge.12037](https://doi.org/10.1111/rge.12037).
- Zamanian, H., Sameti, M., Pazoki, A., Barani, N., and Ahmadnejad, F., 2017, Thermobarometry in the Sarvian Fe-skarn deposit (Central Iran) based on garnet–pyroxene chemistry and fluid inclusion studies: *Arabian Journal of Geosciences*, v. 10, no. 3. doi:[10.1007/s12517-016-2785-z](https://doi.org/10.1007/s12517-016-2785-z).
- Zanchetta, S., Zanchi, A., Villa, I., Poli, S., and Muttoni, G., 2009, The Shanderman eclogites: A Late Carboniferous high-pressure event in the NW Talesh Mountains (NW Iran): *Geological Society*, volume Vol. 312: London, Special Publications, p. 57–78. doi:[10.1144/SP312.4](https://doi.org/10.1144/SP312.4).
- Zanchi, A., Zanchetta, S., Berra, F., Mattei, M., Garzanti, E., Molyneux, S., Nawab, A., and Sabouri, J., 2009, The Eo-Cimmerian (Late Triassic?) orogeny in North Iran: *Geological Society*, London, Special Publications, v. 312, p. 31–55. doi:[10.1144/SP312.3](https://doi.org/10.1144/SP312.3).
- Zandifar, S., Valizadeh, M.V., and Barghi, M.A., 2008, Origin of Garnet zoning in the contact metamorphic areole of Hassan-Abaad intrusion, southwest of Taft: *Economic Geology*, v. 1, p. 71–82. (in Persian). doi:[10.22067/econg.v1i1.3682](https://doi.org/10.22067/econg.v1i1.3682).
- Zarasvandi, A., Liaghat, S., Zentilli, M., and Reynolds, P.H., 2007, ⁴⁰Ar/³⁹Ar Geochronology of Alteration and Petrogenesis of Porphyry Copper Related Granitoids in the Darreh-Zerreshk and Ali-Abad area, Central Iran: *Exploration and Mining Geology*, v. 16, p. 11–24. doi:[10.2113/gsemg.16.1-2.11-a](https://doi.org/10.2113/gsemg.16.1-2.11-a).
- Zhang, J., Changqian, M. C., and She, Z., 2012, An Early Cretaceous garnet-bearing metaluminous A-type granite intrusion in the East Qinling Orogen, central China: Petrological, mineralogical and geochemical constraints: *Geoscience Frontiers*, p. 1–12. doi:[10.1016/j.gsf.11.011](https://doi.org/10.1016/j.gsf.11.011).